Article:
Garrido, Mercedes María, Landon, Malena, Sabbadin, Federico et al. (5 more authors) (2020) PsAA9A, a C1-specific AA9 lytic polysaccharide monooxigenase from the white-rot basidiomycete Pycnoporus sanguineus. APPLIED MICROBIOLOGY AND BIOTECHNOLOGY. ISSN 0175-7598

https://doi.org/10.1007/s00253-020-10911-6

Applied Microbiology and Biotechnology

PsAA9A, a C1-specific AA9 lytic polysaccharide monooxigenase from the white-rot basidiomycete Pycnoporus sanguineus

--Manuscript Draft--

Manuscript Number:	AMAB-D-20-01716R1
Full Title:	PsAA9A, a C1-specific AA9 lytic polysaccharide monooxigenase from the white-rot basidiomycete Pycnoporus sanguineus
Article Type:	Original Article
Section/Category:	Biotechnologically relevant enzymes and proteins
Corresponding Author:	Eleonora Campos Instituto Nacional de Tecnologia Agropecuaria Hurlingham, Buenos Aires ARGENTINA
Corresponding Author Secondary Information:	
Corresponding Author's Institution:	Instituto Nacional de Tecnologia Agropecuaria
Corresponding Author's Secondary Institution:	
First Author:	Mercedes María Garrido, Molecular Biologist
First Author Secondary Information:	
Order of Authors:	Mercedes María Garrido, Molecular Biologist
	Malena Landoni, PhD
	Federico Sabbadin, PhD
	María Pía Valacco, PhD
	Alcia Couto, PhD
	Neil Charles Bruce, PhD
	Sonia Alejandra Wirth, PhD
	Eleonora Campos
Order of Authors Secondary Information:	
Funding Information:	Agencia Nacional de Promoción Científica y Tecnológica (PICT 2016-4695) — Dr. Eleonora Campos
	Secretaria de Ciencia y Tecnica, Universidad de Buenos Aires (20020130100476BA) — Dr Sonia Alejandra Wirth
Abstract:	Woody biomass represents an important source of carbon on earth and its global recycling is highly dependent on Agaricomycetes fungi. White-rot basidiomycetes are a very important group in this regard, as they possess a large and diverse enzymatic repertoire for biomass decomposition. Among these enzymes, the recently discovered lytic polysaccharide monooxygenases (LPMOs) have revolutionized biomass processing with their novel oxidative mechanism of action. The strikingly high representation of LPMOs in fungal genomes raises the question of their functional versatility. In this work, we studied an AA9 LPMO from the white-rot basidiomycete Pycnoporus sanguineus , Ps AA9A. Successfully produced as a recombinant secreted protein in Pichia pastoris , Ps AA9A was found to be a C1-specific LPMO active on cellulosic substrates, generating native and oxidized cello-oligosaccharides in the presence of an external electron donor. Ps AA9A boosted cellulolytic activity of glysoside hydrolases from families GH1, GH5, and GH6.This study serves as a starting point towards understanding the functional versatility and biotechnological potential of this enzymatic family, highly represented in wood decay fungi, in Pycnoporus genus.

Dear Editor,

We are hereby submitting our article "*Ps*AA9A, a C1-specific lytic polysaccharide monooxigenase from the white-rot basidiomycete *Pycnoporus sanguineus* active on cellulose and β-chitin" to be considered for publication in Applied Microbiology and Biotechnology.

The enzyme presented in this work is the first AA9 from *P. sanguineus* to be characterized and is the first C1-selective AA9 that has been shown to have activity on a substrate other than cellulose (β-chitin). It has activity at moderate pH and temperature, as a difference to other fungal enzymes that act preferably at higher temperatures and lower pH.

We have also demonstrated that it presented synergy with cellobiohydrolases or exoglucanases (CBHII and CBHI), endoglucanses and even with β-glucosidases, improving significantly the conversion of the polysaccharide cellulose to cellobiose or glucose (in the case of β-glucosidases). Moreover, we have confirmed that boosting interaction with GH7 can be negatively affected in the presence of small phenolic compounds, as it has been suggested in previous work.

These are crucial aspects for developing novel enzymatic cocktails, tailor-made for specific processes.

All authors have revised and approved the new version of the manuscript.

We look forward to your response.

With our best regards,

Dr. Eleonora Campos (corresponding author).

*Ps*AA9A, a C1-specific AA9 lytic polysaccharide monooxygenase from the white-rot basidiomycete *Pycnoporus sanguineus*

Mercedes María Garrido[1,2], Malena Landoni[3], Federico Sabbadin[4], María Pía Valacco[5], Alicia Couto[3], Neil Charles Bruce[4], Sonia Alejandra Wirth[2], Eleonora Campos[1]

1- Instituto de Agrobiotecnología y Biología Molecular (IABIMO), Instituto Nacional de Tecnología Agropecuaria (INTA-CONICET). Los Reseros y Nicolas Repetto s/n (1686), Hurlingham, Buenos Aires, Argentina.
2- Laboratorio de Agrobiotecnología, Instituto de Biodiversidad y Biología Experimental y Aplicada (IBBEA) CONICET-UBA, Facultad de Ciencias Exactas y Naturales, Universidad de Buenos Aires (C1428EG), Buenos Aires, Argentina.
3- Centro de Investigación en Hidratos de Carbono (CIHIDECAR), Facultad de Ciencias Exactas y Naturales, Universidad de Buenos Aires (C1428EG), Buenos Aires, Argentina.
4- Centre for Novel Agricultural Products (CNAP), Department of Biology, University of York, York YO10 5DD, UK.
5- Instituto de Química Biológica (IQUIBICEN), Facultad de Ciencias Exactas Y Naturales, Universidad de Buenos Aires (C1428EG), Buenos Aires, Argentina.

Corresponding author: Eleonora Campos (campos.eleonora@inta.gob.ar)
Other authors: garrido.mercedes@inta.gob.ar; mlandoni@qo.fcen.uba.ar; federico.sabbadin@york.ac.uk; pvalacco@qb.fcen.uba.ar; acouto@qo.fcen.uba.ar; neil.bruce@york.ac.uk; sonia.wirth@gmail.com

KEY WORDS
Pycnoporus; LPMO; AA9; CELLULOSE

ABSTRACT
Woody biomass represents an important source of carbon on earth and its global recycling is highly dependent on *Agaricomycetes* fungi. White-rot *basidiomycetes* are a very important group in this regard, as they possess a large and diverse enzymatic repertoire for biomass decomposition. Among these enzymes, the recently discovered lytic polysaccharide monooxygenases (LPMOs) have revolutionized biomass processing with their novel oxidative mechanism of action. The strikingly high representation of LPMOs in fungal genomes raises the question of their functional versatility. In this work, we studied an AA9 LPMO from the white-rot basidiomycete *Pycnoporus sanguineus*, *Ps*AA9A. Successfully produced as a recombinant secreted protein in *Pichia pastoris*, *Ps*AA9A was found to be a C1-specific LPMO active on cellulosic substrates, generating native and oxidized cello-oligosaccharides in the presence of an external electron donor. *Ps*AA9A boosted cellulolytic activity of glysoside hydrolases from families GH1, GH5, and GH6.This study serves as a starting point towards understanding the functional versatility and biotechnological potential of this enzymatic family, highly represented in wood decay fungi, in *Pycnoporus* genus.

KEY POINTS
*Ps*AA9A is the first AA9 from *P. sanguineus* to be characterized.
*Ps*AA9A has activity on cellulose, producing C1-oxidized cello-oligosaccharides.
Boosting activity with GH1, GH5 and GH6 was proven.

INTRODUCTION

Agaricomycetes fungi are the major decomposers of organic matter and dominate the recycling of its sequestered carbon. Within this class of *basidiomycetes*, wood-decaying fungi follow different strategies for lignocellulose decomposition using a diverse plethora of hydrolytic and oxidative enzymes as well as non-enzymatic processes. The most representative order of *Agaricomycetes* causing wood decay is the *Polyporales*, which includes the genus *Pycnoporus* with four worldwide distributed species that cause wood decay by white rot, meaning that they are able to efficiently mineralize the lignin of plant cell walls (Lundell et al. 2010). *Pycnoporus* species have been recognized for their biotechnological potential because they synthesize high value-added compounds (Falconnier et al. 1994; Asther et al. 1998; Alvarado et al. 2003) and carbohydrate active enzymes with remarkable thermal stability and broad pH range activity

(Lomascolo et al. 2011; Falkoski et al. 2012; Niderhaus et al. 2018). In addition, the high efficiency of *Pyncoporus* species for the decomposition of hard and soft wood has generated a growing interest in the study of the enzymes involved and the correlating mechanisms (Levin et al. 2007; Levasseur et al. 2014; Couturier et al. 2015). Comparative transcriptomic and secretomic analysis of *Pyncoporus sanguineus* grown in complex plant materials allowed the identification of differentially expressed genes and the corresponding secreted proteins (Miyauchi et al. 2016). In subsequent work, the same authors compared the transcriptomic and secretomic expression patterns at different time points in response to different lignocellulosic substrates of *Pyncoporus coccineus*, a very closely related fungus. The study concluded that genes encoding enzymes associated with a Carbohydrate Binding Module (CBM1) were strongly up-regulated and that there was a close involvement of AA9 lytic polysaccharide monooxigenases (LPMOs) in adaptive responses of the fungi to complex substrates (Miyauchi et al. 2017). Of the 16 AA9 LPMOs identified in *P. sanguineus* genome, none have been characterized to date.

LPMOs are metalloenzymes that bind a copper atom through a characteristic and highly conserved histidine brace (Quinlan et al. 2011). An external electron donor reduces the copper provoking a reaction between the enzyme with either O_2 or H_2O_2 and consequently a powerful oxygen species is created which can then oxidize and break the glycosidic bond either at the C1 or C4 position (Eijsink et al. 2019). LPMOs are currently classified by CAZY as Auxilliary Active Enzymes (AA) (Levasseur et al. 2013) and, to date, make up seven different families (AA9, AA10, AA11, AA13, AA14, AA15 and AA16) based on sequence similarity. Interestingly, the active site is typically positioned on a flat surface (Karkehabadi et al. 2008) which enables the enzyme to oxidize crystalline polysaccharides (Aachmann et al. 2012), making them more accessible to glycoside hydrolases (GHs) and playing a crucial role in polysaccharide degradation (Harris et al. 2010; Vaaje-Kolstad et al. 2010; Muller et al. 2015). Cellulose-active AA9 LPMOs show different regioselectivities producing either C1-oxidized products (lactones, that spontaneously convert to aldonic acids), C4-oxidized products (ketones, that spontaneously convert to gemdioles), or a mixture of both (Vaaje-Kolstad et al. 2017). In recent years, a lot of effort has been dedicated into finding phylogenetic relationships between regioselectivity, substrate specificity and amino acid sequence of AA9 LPMOs (Li et al. 2012; Moses et al. 2016) but no determinant feature has been identified yet (Frommhagen et al. 2018). The diversity of AA9s in white-rot fungi is thought to allow wider substrate specificity and biochemical adaptability (Berrin et al. 2017).

The *P. sanguineus* genome was made publicly available in 2014 by the Joint Genome Institute (JGI, Department of Energy, USA) and several transcriptomic and secretomic studies have been carried out on this species and closely related ones (Rohr et al. 2013; Miyauchi et al. 2016; 2017; Zhang et al. 2019). Among 16 putative AA9 LPMOs encoded in *P. sanguineus* genome, this work focuses on *Ps*AA9A. The transcript for *Ps*AA9A (JGI, *P. sanguineus* BRFM 1264 v1.0, transcript ID: 1583829) was the most strongly upregulated in lignocellulose-containing media (Miyauchi et al. 2016) and the only LPMO sequence featuring an appended CBM. Also, the gene encoding *Ps*AA9A has been found to be differentially expressed when *P. sanguineus* was grown in wheat straw as opposed to its growth in maltose. Additionally, it was found to be co-regulated with genes coding for a GH131_CBM1, CBM1_GH6, CBM1_GH5_7, AA8-AA3_1, GH7, GH74, and GH28 (Miyauchi et al. 2016) which suggested that these proteins may act in synergy to degrade this complex substrate.

We present here the first functional characterization of *Ps*AA9A including its regioselectivity, activity in the presence of various electron donors, synergism with canonical GHs and substrate specificity. This study sheds the first light on the biological basis of AA9 multiplicity in this major white-rot genus, and opens up new opportunities for its biotechnological exploitation.

MATERIALS AND METHODS

Cloning of *Ps*AA9A

The full coding sequence for *Ps*AA9A (protein ID: 1583489, JGI) from *P. sanguineus,* including its native signal sequence and without stop codon, was obtained from *P. sanguineus* genome publicly available at Joint Genome Institute portal (https://mycocosm.jgi.doe.gov/Pycsa1/Pycsa1.home.html) and was synthesized for expression in *P. pastoris* using the gene synthesis and codon optimization service by Genescript (Piscataway, USA) (supplied in pUC57 plasmid, cloned in *Eco*RV restriction site). Synthetic

DNA sequence was deposited at GenBank under accession number MT076044. For expression of mature *Ps*AA9A fused to a C-terminal 6xHIS tag in *P. pastoris*, the *Bam*HI/*Spe*I restriction product was cloned into the pPICHIS vector, a derivative of pPIC9 (Invitrogen Life Technologies, Waltham, USA), replacing the α-factor signal sequence to obtain plasmid p*Ps*AA9AHis. Plasmid pPICHIS contains a 6-histidine coding sequence in frame with *Spe*I and followed by a stop codon (Campos et al. 2016).

Prediction of signal peptide and processing site in the translated protein was performed using SignalP 4.0 software (http://www.cbs.dtu.dk/services/SignalP/) and prediction of *N*- and *O*-glycosylation sites with NetNGlyc 1.0 Server (http://www.cbs.dtu.dk/services/NetNGlyc/) and NetOGlyc 4.0 Server (http://www.cbs.dtu.dk/services/NetOGlyc/), respectively.

Recombinant *Ps*AA9A expression in *P. pastoris* and purification

Recombinant vector p*Ps*AA9AHis was linearized with *Bgl*II restriction enzyme and used for transformation of *P. pastoris* strain GS115 (Invitrogen Life Technologies, Waltham, USA) by electroporation. Recombinant clones reverting histidine auxotrophy were selected on minimal medium MD plates (0.34% yeast nitrogen base without amino acids, 10 g/L $(NH_4)_2SO_4$, 2% dextrose and 2% agar). Integration in the AOX1 locus of the *P. pastoris* genome was verified by colony PCR using the universal primers 5'AOX1 (GACTGGTTCCAATTGACAAGC) and 3'AOX1 (GCAAATGGCATTCTGACATCC) (Linder et al. 1996). Single colonies were suspended in 100 µL sterile water and incubated with 15 U of Lyticase from *Arthrobacter luteus* (Sigma Aldrich, Saint Louis, USA) for 30 min at 37°C, boiled for 5 min and the DNA was recovered by centrifugation at 12000 g for 5 min. PCR amplifications were performed in 50 µL volumes reaction with 15 µL of DNA template, 50 pmol of each primer, 0.2 mM of each dNTP, 2 mM $MgCl_2$, 1 unit of Taq polymerase and 1X reaction buffer (Invitrogen Life Technologies, Waltham, USA). After an initial denaturation of 3 min at 95°C, the amplification was carried out for 30 cycles of 95°C, 30 sec; 60°C, 30 sec and 72°C, 2.5 min and a final single step of 72°C, 10 min. Positive clones were selected and conserved on MD or YPD (1% yeast extract, 2% peptone, 2% dextrose, 2% agar) agar slants.

Histidine tagged recombinant protein production in *P. pastoris* and purification by Ni-NTA affinity chromatography was performed in the same conditions as previously described (Campos et al. 2016). Briefly, pre-inoculums were generated in 5 mL of YPD medium and 1 mL was used as seed to inoculate 80 mL of BMGY (1% yeast extract, 2% peptone, 0.34% yeast nitrogen base without amino acids, 10 g/L $(NH_4)_2SO_4$, 400 mg/L biotin, 4% glycerol, 100 mM potassium phosphate buffer, pH 6.0) in 500 mL shake flasks and cultivated for 48 h at 30°C and 220 rpm. Cells were harvested by centrifugation 5 min at 1500 g and resuspended in 300 mL of BMMY medium (1% yeast extract, 2% peptone, 100 mM potassium phosphate buffer, pH 6.0, 0.34% yeast nitrogen base without amino acids, 10 g/L $(NH_4)_2SO_4$, 400 mg/L biotin) to a final OD600 nm = 2.5 and cultivated in 1 L shake flasks at 28°C and 220 rpm. Sterile methanol (0.5% final) was added every 24 h to maintain induction conditions.

P. pastoris cultures were harvested after 4 days of induction and centrifuged at 1500 g for 10 min. The supernatant was concentrated by ultrafiltration (30 kDa MWCO, Amicon Ultra. Merck Millipore, Burlington, USA) and buffer exchanged to equilibration buffer (300 mM NaCl, 50 mM sodium phosphate buffer, pH 8). Recombinant *Ps*AA9A was purified by gravity flow Ni-NTA affinity chromatography using His select nickel affinity gel (Sigma Chemical Co., Saint Louis, USA). In order to saturate the active site with copper, 5-fold molar excess of a 20 mM $CuSO_4$ solution was decanted into the protein solution while mixing gently to avoid precipitation and then loaded into a HiLoad 16/60 Superdex 75 prep grade column (GE Healthcare, Chicago, USA) for size exclusion chromatography, to remove salts and unbound copper. The purified protein was eluted from the column in 20 mM sodium phosphate buffer pH 7. The resulting yield was 7.5 mg of purified copper-saturated protein obtained from a 1 L culture.

Polyacrylamide gel electrophoresis and immunoblotting

Recombinant *Ps*AA9A in crude cell-free extracts was separated by reducing 12% SDS-PAGE and identified by Coomassie Blue staining or transferred to 0.45 µm nitrocellulose membrane (Bio-Rad Laboratories Inc, Hercules, USA). Western blot was performed by probing the membrane with 0.1 µg/mL of polyclonal rabbit anti-HIS antibody (Genescript, Piscataway, USA) followed by 1:15000 dilution of alkaline phosphatase-linked goat anti-rabbit antibody (Sigma Chemical Co., Saint Louis, USA). Phosphatase activity was revealed by a chromogenic reaction using 5-bromo-4-chloro-3-indolyl phosphate (BCIP) and nitroblue tetrazolium (NBT) as substrates (Sigma Chemical Co., Saint Louis, USA).

Thermal shift assay (Thermofluor)

SyPro orange protein gel stain (Invitrogen Life technologies S6650, Waltham, USA) reactant was added to 5 µM *Ps*AA9A alone or in the presence of 10 mM EDTA and thermofluor assay was conducted using an Mx3005P qPCR System (Agilent Technologies, Santa Clara, USA). The intensity of the fluorescence was measured at a temperature gradient (25°C - 90°C with 1°C intervals) and converted into a melting curve to determine the melting temperature (Tm).

Proteomic analysis

Purified *Ps*AA9A was quantified by Bradford assay (Promega, Biodynamics, CABA, Argentina), then precipitated with 10% trichloro acetic acid (TCA) and resuspended in water (18 Ω) to a final concentration of 1 mg/mL. Protein digestion and mass spectrometry analysis were performed at CEQUIBIEM (http://cequibiem.qb.fcen.uba.ar/). The protein sample was reduced with dithiotreitol 10 mmol/L for 45 min at 56 °C, alkylated with iodo acetamide (55 mmol/L) for 45 min in the dark and digested with trypsin (Promega V5111; Promega, Fitchburg, WI) overnight at 37°C. The digests were analyzed by nano LC-MS/MS in a Thermo Scientific Q-Exactive Mass Spectrometer coupled with a nano HPLC EASY-nLC 1000 (Thermo Fisher Scientific, CABA, Argentina). For the LC-MS/MS analysis, approximately 1 µg of peptides was loaded onto the column and eluted for 120 min using a reverse phase column (C18, 2 lm, 100 A, 50 lm 9 150 mm) Easy-Spray Column PepMap RSLC (P/N ES801) suitable for separating complex peptide mixtures with a high degree of resolution. The flow rate used for the nano column was 300 nL/min and the solvent range from 7% B (5 min) to 35% (120 min). Solvent A was 0.1% formic acid in water, whereas B was 0.1% formic acid in acetonitrile. The injection volume was 2 µL. A voltage of 3.5 kV was used for Electro Spray Ionization (Thermo Fisher Scientific; EASYSPRAY, Thermo Fisher Scientific, CABA, Argentina). The MS equipment has a high collision dissociation cell (HCD) for fragmentation and an Orbitrap analyser (Thermo Fisher Scientific; Q-Exactive, Thermo Fisher Scientific, CABA, Argentina). XCALIBUR3.0.63 (Thermo Fisher Scientific, Thermo Fisher Scientific, CABA, Argentina) software was used for data acquisition and equipment configuration to allow simultaneous chromatographic separation and peptide identification. Full-scan mass spectra were acquired in the Orbitrap analyser. The scanned mass range was 400–2,000 m/z, at a resolution of 70,000 at 400 m/z, and the 12 most intense ions in each cycle, were sequentially isolated, fragmented by HCD and measured in the Orbitrap analyser. Peptides with a charge of +1 or with unassigned charge state were excluded from fragmentation for MS2. Q Exactive raw data was processed using Proteome Discoverer software (version 2.1.1.21 Thermo Scientific, Thermo Fisher Scientific, CABA, Argentina) and searched against the expected sequences, with trypsin specificity and a maximum of one missed cleavage per peptide. Carbamidomethylation of cysteine residues was set as a fixed modification and oxidation of methionine was set as variable modification, a precursor mass tolerance of 10 ppm and product ion tolerance to 0.05 Da. No-enzyme searches were also performed to analyze the N-terminal portion of the protein.

In vitro activity assays

Typical reactions for *Ps*AA9A characterization were carried out by mixing 1-5 mg/mL PASC with 1-2 µM purified protein, 1-4 mM electron donor (ascorbic or gallic acid), in a total volume of 100 µL in 2 mL plastic reaction tubes. The other substrates (avicel, β-chitin, pachyman, glucomannan, galactomannan, lichenan, xyloglucan, xylan from beechwood, and α-chitin) and electron donors (pyrogallol, caffeic acid, ferulic acid and *p*-coumaric acid) tested were used in the same conditions. All reactions analyzed via MALDI-TOF were carried out in 50 mM ammonium acetate buffer pH 6 and incubated at 30°C shaking at 600 rpm and the supernatant used for analysis.

Reactions used for product quantification and synergism experiments with *Ps*AA9A were typically carried out in 50 mM sodium phosphate buffer pH 6 in triplicates of 100 µL each for 3 h at 30°C at 600 rpm. Each reaction contained 2 µM purified *Ps*AA9A, 1–4 mg/mL PASC, and 1 mM gallic acid. Commercial GH1 (4 mU; cat. Number E-BGOSAG, Megazyme, Bray, Ireland), GH5 (6 mU; cat. number E-CELBA, Megazyme, Bray, Ireland), GH6 (0.8 mU; cat. number E-CBHIIM, Megazyme, Bray, Ireland), and GH7 (0.1 mU; cat. number E-CBHI, Megazyme, Bray, Ireland) were added to 100 µL reactions. After 3 h incubation, 400 µL of ethanol were added to stop the reaction, spun down and 400 µL of supernatant was transferred

to new plastic tubes, dried down and re-suspended in 160 µL of pure water, filtered and analyzed via HPAEC-PAD.

In all cases, controls of substrate with and without electron donor (without enzyme) and substrate with enzyme (without electron donor) were included in the analysis.

Product analysis by HPAEC-PAD

Oligosaccharides were analyzed via High-performance Anion Exchange Chromatography (HPAEC) using a ICS-3000 Pulsed Amperometric Detection (PAD) system with an electrochemical gold electrode, a CarboPac PA20 3 × 150 mm analytical column and a CarboPac PA203 × 30 mm guard column (Dionex, Thermo Fisher Scientific, CABA, Argentina). Sample aliquots of 5 µL were injected and separated at a flow rate of 0.5 mL/min at a constant temperature of 30 °C. After equilibration of the column with 50% H_2O-50% 0.2 M NaOH, a 30-min linear gradient was started from 0% to 20% with 0.5 M sodium acetate in 0.2 M NaOH and then kept constant for 20 min. The column was then washed with 0.2 M NaOH for 6 min and re-equilibrated for 4 min with 50% H_2O-50% 0.2 M NaOH before starting the next run (oligosaccharide method).

Glucose was analyzed with the following HPAEC program (monosaccharide method). After equilibration of the column with 100% H_2O, sample aliquots of 5 µL were injected and separated at a flow rate of 0.5 mL/min at a constant temperature of 25 °C. The column was washed with 100% H_2O for 10 min, followed by 9 min of 99% H_2O-1% 0.2 M NaOH. The column was then washed with 0.2 M NaOH for 6 min and re-equilibrated with 100% H_2O before injection of the next sample. Integrated peak areas were compared to mono and oligo-saccharide calibration standards (glucose, cellobiose, cellotriose, cellotetraose, cellopentaose, cellohexaose, *N*-acetylglucosamine, chitobiose, chitotriose, chitotetraose, chitopentaose) purchased from Megazyme (Bray, Ireland). C1 oxidized cellobiose standard was chemically synthesized as described in the following section.

Synthesis of C1 oxidized cellobiose standard

The cellobiose was chemically oxidized as previously described (Forsberg et al. 2011) using a mild oxidation method that has been shown to selectively oxidize the hemiacetal carbon of carbohydrates to generate aldonic acids (Kobayashi et al. 1985 and 1996). Briefly, the cellobiose (0.2 g) was dissolved in 2 mL water and mixed with an iodine solution (7.3 mmol iodine in 15 mL methanol). While stirring, 5 mL of a 4% (w/w) solution of KOH in methanol was added dropwise for 5 min and then the reaction was kept at room temperature for 30 min. The solution was heated to 40°C for 1 h until the color disappeared. Cooling in the refrigerator overnight yielded a precipitate of white crystals that was filtered and washed with cold methanol. The solid was redissolved in 2 mL water. The product was analyzed by HPAEC-PAD in the same conditions described above.

Product analysis by mass spectrometry

One microliter of reaction supernatant was mixed with an equal volume of 20 mg/mL 2,5-dihydroxybenzoic acid (DHB) in 50% acetonitrile, 0.1% TFA on a SCOUT-MTP 384 target plate (Bruker, Billerica, USA). The spotted samples were then dried in a vacuum desiccator before being analyzed by mass spectrometry on an Ultraflex III matrix-assisted laser desorption ionization time of flight/time of flight (MALDI/TOF-TOF) instrument (Bruker, Billerica, USA) (Abdul Rahman et al. 2014).

RESULTS

In silico and phylogenetic analysis of *Ps*AA9A

In silico analysis of *Ps*AA9A showed the presence of an N-terminal signal peptide for secretion, and conserved residues (His 1, His 80, Tyr 167, of the mature protein) involved in copper coordination within the catalytic site (Fig. 1a). A CBM1, containing four conserved cysteine residues involved in disulfide bridge formation and the conserved aromatic residues (Y4, Y30 and Y31) involved in ligand recognition (Gilkes et al. 1991, Varnai et al. 2014), is located at C-terminus linked to the catalytic domain by a flexible linker rich in proline-threonine residues. Phylogenetic analysis of the mature catalytic domain of *Ps*AA9A and other biochemically characterized AA9 LPMOs placed *Ps*AA9A in a cluster together with *Hi*LPMOB

(GenBank ETW87087.1) and *Mt*PMO3 (GenBank AEO56665.1), both C1-specific AA9 LPMOs from the white-rot basidiomycete *Heterobasidion irregulare* and the ascomycete *Myceliophthora thermophila* respectively (Fig. 1b). Alignment of *Ps*AA9A with *Hi*LPMOB and *Mt*PMO3 revealed that *Ps*AA9A has several features that were shown to be present in *Hi*LPMOB and *Mt*PMO3 but not in other C1-specific LPMOs (Supplemental Fig. S1). These three enzymes have a longer L2 loop (10-aminoacid extension) with an aromatic residue in position 20 and a Tyr residue (Tyr36 in *Ps*AA9A) that were found to be located on the substrate binding surface in the vicinity of the active-site copper (Liu et al. 2018) (Fig. 1a). Moreover, they have a shorter L3 loop devoid of a conserved Tyr residue, replaced by Pro79 in *Ps*AA9A and *Hi*LPMOB, and Tre74 in *Mt*PMO3.

Recombinant *Ps*AA9A produced in *P. pastoris*

*Ps*AA9A was successfully produced from *P. pastoris* transformants and secreted to the extracellular media with an apparent molecular mass higher than the theoretical one (55 and 31.27 KDa, respectively) (Supplemental Fig. S2), which could be explained by the presence of a potential *N*-glycosylation site at position 134 of the mature protein and to *O*-glycosylation in the serine/threonine rich linker region between the catalytic module and the CBM1 (Langsford et al. 1987; Abuja et al. 1988). Mass spectrometry analysis revealed the presence of correctly processed mature protein containing the N-terminal His catalytic residue. However, peptides retaining three additional amino acids from the signal peptide in the N-terminal portion of the protein were also detected. This can be related to random incorrect processing of foreign signal peptides, which has also been recently reported for other recombinant LPMOs expressed in *P. pastoris* (Jagadeeswaran et al. 2018; Eijsink et al. 2019).

Thermal shift analysis of the *Ps*AA9A copper-saturated protein indicated a melting temperature (Tm) of 47.9°C, which decreased to 46.3°C upon addition of 10 mM EDTA, indicating that copper binding to the active site increased protein thermal stability, as previously observed for other LPMOs such as *Td*AA15A (Sabbadin et al. 2018) (Supplemental Fig. S3).

***Ps*AA9A acts with C1-oxidative regioselectivity**

Based on the fact that AA9 LPMOs characterized to date are mainly known for being active on crystalline cellulose and that the protein in study is fused to a CBM1 module (which usually binds cellulose), we first evaluated the activity and regioselectivity of *Ps*AA9A on Phosphoric Acid Swollen Cellulose (PASC), using ascorbic acid as electron donor. After 24 hours of incubation, soluble reaction products were analyzed by mass spectrometry (MALDI-TOF) and HPAEC-PAD revealing peaks corresponding to native and C1-oxidized cello-oligosaccharides (COS) with degrees of polymerization (DP) 2 to 5 (Fig. 2). Commercial native COS and in-house chemically synthesized C1-oxidized cellobiose were used as standards for HPAEC-PAD analysis. Similar reactions were carried out at different temperatures (30, 40, 45, 50 and 60 °C) and pH (5, 5.5, 6 and 7.5) releasing native and oxidized COS in all the conditions tested, demonstrating the versatility of the enzyme. (Supplemental Fig. S4). The above-mentioned peaks were not present in control reactions without LPMO tested for every condition (data not shown). No peaks compatible with C4-oxidation were observed. These results confirmed that recombinant *Ps*AA9A was purified in an active form and that it is a cellulose C1-oxidative enzyme (EC 1.14.99.54).

Electron donors and substrate specificity for *Ps*AA9A

In nature, LPMOs require molecular oxygen and an extracellular electron source, which could be supplied enzymatically, i.e. by cellobiose dehydrogenase (CDH), or by small molecule reductants present in the lignocellulosic biomass. A set of compounds that could act as electron donors was assayed using PASC as substrate and soluble reaction products were analyzed by MALDI-TOF. Control reactions were performed without electron donor and without LPMO, separately. C1-oxidized oligosaccharides were detected when using ascorbic acid and the phenolic compounds gallic acid, pyrogallol, caffeic acid, and ferulic acid but not with *p*-coumaric acid (Supplemental Fig. S5), proving that a wide range of small phenolic compounds could act as electron donors.

For substrate specificity assays, gallic acid was selected as electron donor, as it was previously described to be more stable than ascorbic acid in oxygenated buffers at pH 6 (Kracher et al. 2016). As expected, *Ps*AA9A was active on the cellulosic substrates Avicel (crystalline cellulose) and PASC. However, we also observed activity on squid β-chitin, which

had not been previously reported for AA9 LPMOs (Fig. 3). This activity was also detected when using ascorbic acid as electron donor. Control reactions for β-chitin alone and with electron donor were performed (Supplemental Fig. S6). Other polysaccharide substrates with varying glycosidic linkages were tested including pachyman, glucomannan, galactomannan, lichenan, xyloglucan, xylan from beechwood, and α-chitin, but the release of native and oxidized oligosaccharides was not detected in these cases (Table 1).

*Ps*AA9A boosts the activity of commercial cellulases

In order to test the synergic potential of *Ps*AA9A with cellulases for the deconstruction of cellulose, it was assayed on PASC, in co-incubation experiments with individual commercial cellulases (GH6 cellobiohydrolase II, GH7 cellobiohydrolase I, GH5 endoglucanase, or GH1 β-glucosidase) and the released products were quantified by HPAEC-PAD. The concentration of commercial enzymes was selected to release quantifiable products by themselves, without saturating the reaction, to be able to monitor a potential increase (see materials and methods). Experiments were carried out for 3 h, as COS release was not detected by *Ps*AA9A alone at this time point in a time-course assay (Supplemental Fig. S7). Synergism indexes (SI) were calculated comparing glucose (in the case of GH1) or cellobiose concentration (μM) in the soluble products of the individual and combined reactions. High SI were detected when *Ps*AA9A was co-incubated with GH1, GH5, and GH6, demonstrating a boosting effect in the activity of the individual glycoside hydrolases (Fig. 4a-c). Noteworthy, although there was a boosting effect in cellobiose release when GH7 cellobiohydrolase I was supplemented with *Ps*AA9A, an inhibition was observed in the presence of 1 mM gallic acid (Fig.4d) which can be explained by gallic acid partial inhibition of GH7 activity under the assay conditions (Supplemental Fig. S8).

DISCUSSION

Although an outstanding number of in silico data on fungal genomes, transcriptomes and secretomes have been published in the past decade (Aguilar-Pontes et al. 2014; Grigoriev et al. 2014) the processing and biological analysis of this information is lagging far behind.

The strikingly high representation of AA9s in fungal genomes (Bennati-Granier et al. 2015; Berrin et al. 2017; Berlemont, 2017) and the big sequence diversity found within this family (Vaaje-Kolstad et al. 2017; Frommhagen et al. 2018; Hemsworth et al. 2015) suggests a wide versatility of their mechanism of action and substrate specificity which may result in better adaptations to different environments. Among the seven published LPMO families, proteins of family AA9 show the largest variation in substrate specificity (Frommhagen et al. 2018). Moreover, AA9 LPMOs have different regioselectivities that can generate polysaccharide chain breaks resulting from oxidation at C1, C4, or at both carbon atoms of a sugar ring (Vaaje-Kolstad et al. 2010; Quinlan et al. 2011; Hemsworth et al. 2015).

P. sanguineus has 16 putative AA9 family LPMOs encoded in its genome. Among these, *Ps*AA9A was the only upregulated AA9 transcript when the fungus was grown on wheat straw biomass (Miyauchi et al. 2016) and it is the only one appended to a CBM1. CBM1 modules, which are found almost exclusively in fungi, show affinity towards cellulose but binding to chitin has also been described in one case (Rooijakkers et al. 2018). Previous studies have shown that LPMOs linked to a CBM release more cello-oligosaccharides from cellulose compared to LPMOs without a CBM (Bennati-Granier et al. 2015; Crouch et al. 2016).

When incubated with the cellulosic substrates (PASC and Avicel), *Ps*AA9A generated native and C1-oxidized cello-oligosaccharides, proving its lytic C1-specific oxidative activity on cellulose. Not surprisingly, sequence alignment and phylogenetic analysis of *Ps*AA9A alongside characterized AA9 LPMOs (reported in CAZY database) placed it in the same cluster as C1-oxidizing fungal AA9 LPMOs *Hi*LPMOB from *H. irregulare* and *Mt*PMO3 from *M. thermophila*, further supporting its mechanism of action. Analysis of the 3D structures of *Hi*LPMOB and *Mt*PMO3 (Liu et al. 2018) revealed certain features that differed from other C1-specific AA9 LPMOs, including an extended L2 loop with two aromatic residues, which are also found in *Ps*AA9A. However, the biological implication of this is still unclear. Further activity analysis and structural studies of a higher number of C1-specific enzymes may clarify whether these features could represent an evolutionary adaptation of a subgroup of C1-specific LPMO to substrate binding, as suggested for *Hi*LPMOB and *Mt*PMO3 (Liu et al. 2018).

To date, activity on cellulose was reported for C1, C4 and C1-C4 oxidizing LPMOs, but activity against other polysaccharides such as xylan and mixed-linkage glucans was only reported for C1-C4 and C4 LPMOs (Liu et al. 2018; Frommhagen et al. 2018;). Enzymes that

oxidize exclusively at C1 have only shown activity on cellulose (Frommhagen et al. 2016; Bennati-Granier et al. 2015; Liu et al. 2017). In this regard, *Ps*AA9A was not active on several non-cellulosic substrates (such as xylan, glucomannan and α-chitin) but we observed peaks compatible with oxidized chito-oligosaccharides (CHOS) with DP 5 to 10 released from squid β-chitin, an activity only reported so far for LPMOs of families AA10, AA11 and AA15, being fungal enzymes exclusively from family AA11 (Vaaje-Kolstad et al. 2019). Nevertheless, further studies will be necessary to confirm and characterize the activity on chitin.

The discovery of LPMOs has had a major impact in the way we understand enzymatic conversion of polysaccharides, mainly due to their ability to boost the activity of classical hydrolytic enzymes by enhancing substrate accessibility (Vaaje-Kolstad et al. 2010; Harris et al. 2010). *Ps*AA9A showed synergistic activity with a commercial GH1 β-glucosidase, a GH5 endoglucanase, and a GH6 cellobiohydrolase II, a result in accordance with previous transcriptomic and secretomic data from biomass-grown fungus (Miyauchi et al. 2016), where *Ps*AA9A was co-expressed with several GHs, including a GH5 and a GH6. We did not observe an increase of GH7 cellobiohydrolase I activity on PASC by addition of *Ps*AA9A when small phenolic electron donor, such as gallic acid, was present. Moreover, GH7 activity was lower in the presence of gallic acid (without *Ps*AA9A). These results were in accordance to previous reports that described the inhibition of GH activity by phenolic compounds (Berlin et al. 2006), which was higher for CBH I than for endoglucanases or β-glucosidases (Guo et al. 2014; Mhlongo et al. 2015). Therefore, boosting with exo-glucanases was higher in the case of non-reducing acting enzymes (such as GH6) than with reducing-end acting enzymes such as GH7, which could have further implications when supplementing fungal enzymatic cocktails that have a high abundance of GH7.

The findings presented in this work are relevant to the better understanding of the complex machinery that *P. sanguineus* utilizes for biomass decomposition, which includes this AA9 LPMO.

DECLARATIONS

Funding

This work was supported by Grants PICT2016-4695 (from the National Agency for Science and Technology Promotion from Argentina, ANPCyT) and Grant 20020130100476BA (from the University of Buenos Aires). The Ultraflex II (Bruker, Billerica, USA) TOF/TOF mass spectrometer was supported by ANPCyT Grant PME 125 (CEQUIBIEM). ML, AC, MPV, SAW and EC are Research Career Scientists of the National Research Council of Argentina (CONICET). NCB and EC acknowledge funding from the N8 AgriFood catalyst programme.

Conflict of interests

The authors declare no financial or commercial conflict of interest.

Availability of data and material

Data of *P. sanguineus* *Ps*AA9A synthetic coding sequence was deposited at DDBJ/EMBL/GenBank under the accession number MT076044.

Code availability

Not applicable.

Authors' contributions

EC, NCB and SW conceived and designed research. MG, ML and FS conducted experiments. PV and AC contributed analytical tools and analyzed data. MG wrote the manuscript. All authors read and approved the manuscript.

AKNOWLEDGEMENTS

Authors thank Dr. Leonardo Gomez and Rachel Hallam for invaluable technical assistance.

REFERENCES

Aachmann FL, Sørlie M, Skjåk-Bræk G, Eijsink VGH, and Vaaje-Kolstad G (2012) NMR structure of a lytic polysaccharide monooxygenase provides insight into copper binding, protein dynamics, and substrate interactions. Proc Natl Acad Sci USA 109(46):18779–18784. http://doi.org/10.1073/pnas.1208822109

Abdul Rahman S, Bergström E, Watson CJ, Wilson KM, Ashford DA, Thomas JR, Ungar D, Thomas-Oates JE (2014) Filter-aided *N*-glycan separation (FANGS): a convenient sample preparation method for mass spectrometric *N*-glycan profiling. J proteome res 13(3):1167–1176. http://doi.org/10.1021/pr401043r

Abuja PM, Schmuck M, Pilz I, Tomme P, Claeyssens M, Esterbauer H (1988) Structural and functional domains of cellobiohydrolase I from *Trichoderma reesei*. Eur Biophys J 15:339-342. http://doi.org/10.1007/BF00254721

Aguilar-Pontes MV, de Vries RP, Zhou M (2014) (Post-)genomics approaches in fungal research. Brief Funct Genomics 13(6):424-439. http://doi.org/10.1093/bfgp/elu028

Alvarado I, Navarro D, Record E, Asther M, Asther M, Lesage-Meessen L (2003) Fungal biotransformation of *p*-coumaric acid into caffeic acid by *Pycnoporus cinnabarinus*: an alternative for producing a strong natural antioxidant. World J Microb Biot 19:157-160. http://doi.org/10.1023/A:1023264200256

Asther M, Lomasco A, Asther S, Moukha S, Lesage-meessen L (1998) Metabolic pathways of biotransformation and biosynthesis of aromatic compounds for flavour industry by the basidiomycete *Pycnoporus cinnabarinus*. Micol Neotrop Apl 11:69-76.

Bennati-Granier C, Garajova S, Champion C, Grisel S, Haon M, Zhou S, Fanuel M, Ropartz D, Rogniaux H, Gimbert I, Record E, Berrin JG (2015) Substrate specificity and regioselectivity of fungal AA9 lytic polysaccharide monooxygenases secreted by *Podospora anserina*. Biotechnol Biofuels 8:90. https://doi.org/10.1186/s13068-015-0274-3

Berlemont R (2017) Distribution and diversity of enzymes for polysaccharide degradation in fungi. Sci Rep 7:222. https://doi.org/10.1038/s41598-017-00258-w

Berlin A, Balakshin M, Gilkes N, Kadla J, Maximenko V, Kubo S, Saddler J (2006) Inhibition of cellulase, xylanase and β-glucosidase activities by softwood lignin preparations. J Biotech 125:198–209. http://doi.org/10.1016/j.jbiotec.2006.02.021

Berrin JG, Rosso MN, Hachem MA (2017) Fungal secretomics to probe the biological functions of lytic polysaccharide monooxygenases. Carbohydr Res 448:155-160. http://doi.org/10.1016/j.carres.2017.05.010

Campos P, Levin L, Wirth S (2016) Heterologous production, characterization and dye decolorization ability of a novel thermostable laccase isoenzyme from *Trametes trogii* BAFC 463. Process Biochem 51: 895–903. http://dx.doi.org/10.1016/j.procbio.2016.03.015

Couturier M, Navarro D, Chevret D, Henrissat B, Piumi F, Ruiz-Dueñas F, Martinez AT, Grigoriev I, Riley R, Lipzen A, Berrin JG, Master E, Rosso MN (2015) Enhanced degradation of softwood versus hardwood by the white-rot fungus *Pycnoporus coccineus*. Biotechnol Biofuels 8:216. http://doi.org/10.1186/s13068-015-0407-8

Crouch LI, Labourel A, Walton PH, Davies GJ, Gilbert HJ (2016) The contribution of non-catalytic carbohydrate binding modules to the activity of lytic polysaccharide monooxygenases. J Biol Chem 291(14):7439–7449. http://doi.org/10.1074/jbc.M115.702365

Eijsink VGH, Petrovic D, Forsberg Z, Mekasha S, Røhr AK, Várnai A, Bissaro B, Vaaje-Kolstad G (2019) On the functional characterization of lytic polysaccharide monooxygenases (LPMOs). Biotechnol Biofuels 12:58. https://doi.org/10.1186/s13068-019-1392-0

Falconnier B, Lapierre C, Lesage-Meessen L, Yonnet G, Brunerie P, Colonna-Ceccaldi B, Corrieu G, Asther M (1994) Vanillin as a product of ferulic acid biotransformation by the white-rot fungus *Pycnoporus cinnabarinus* 1-937: identification of metabolic pathways. J Biotech 37:123-132. http://doi.org/10.1016/0168-1656(94)90003-5

Falkoski DL, Guimarães VM, de Almeida MN, Alfenas AC, Colodette JL, de Rezende ST (2012) Characterization of cellulolytic extract from *Pycnoporus sanguineus* PF-2 and its application in biomass saccharification. Appl Biochem Biotechnol 166:1586–1603. https://doi.org/10.1007/s12010-012-9565-3

Forsberg Z, Vaaje-Kolstad G, Westereng B, Bunæs AC, Stenstrøm Y, MacKenzie A, Sørlie M, Horn SJ, Eijsink VG (2011) Cleavage of cellulose by a CBM33 protein. Protein Sci 20(9):1479-83. http://doi.org/10.1002/pro.689

Frommhagen M, Koetsier MJ, Westphal AH, Visser J, Hinz SW, Vincken JP, van Berkel WJ, Kabel MA, Gruppen H (2016) Lytic polysaccharide monooxygenases from *Myceliophthora thermophila* C1 differ in substrate preference and reducing agent specificity. Biotechnol Biofuels 9(1):186. http://doi.org/10.1186/s13068-016-0594-y

Frommhagen M, Westphal AH, van Berkel WJH, Kabel MA (2018) Distinct substrate specificities and electron‐donating systems of fungal lytic polysaccharide monooxygenases. Front Microbiol 9:1080. http://doi.org/10.3389/fmicb.2018.01080

Gilkes NR, Henrissat B, Kilburn DG, Miller RC Jr, Warren RAJ (1991) Domains in microbial β-1,4-glycanases: sequence conservation, function, and enzyme families. Microbiol Rev 55(2):303-315. PMID: 1886523 PMCID: PMC372816

Grigoriev IV, Nikitin R, Haridas S, Kuo A, Ohm R, Otillar R, Riley R, Salamov A, Zhao X, Korzeniewski F, Smirnova T, Nordberg H, Dubchak I, Shabalov I (2014) MycoCosm portal: gearing up for 1000 fungal genomes. Nucleic Acids Res 42:D699–D704. http://doi.org/10.1093/nar/gkt1183

Guo F, Shi W, Sun W, Li X, Wang F, Zhao J, Qu Y (2014) Differences in the adsorption of enzymes onto lignins from diverse types of lignocellulosic biomass and the underlying mechanism. Biotechnol Biofuels 7(1):38. http://doi.org/doi:10.1186/1754-6834-7-38

Harris PV, Welner D, McFarland KC, Re E, Navarro Poulsen JC, Brown K, Salbo R, Ding H, Vlasenko E, Merino S, Xu F, Cherry J, Larsen S, Lo Leggio L (2010) Stimulation of lignocellulosic biomass hydrolysis by proteins of glycoside hydrolase family 61: structure and function of a large, enigmatic family. Biochemistry 49(15):3305-16. http://doi.org/10.1021/bi100009p

Hemsworth GR, Johnston EM, Davies GJ, Walton PH (2015) Lytic polysaccharide monooxygenases in biomass conversion. Trends Biotechnol 33(12):747-761. http://doi.org/10.1016/j.tibtech.2015.09.006

Jagadeeswaran G, Gainey L,Mort AJ (2018) An AA9-LPMO containing a CBM1 domain in *Aspergillus nidulans* is active on cellulose and cleaves cello-oligosaccharides. AMB Expr 8:171. http://doi.org/10.1186/s13568-018-0701-5

Karkehabadi S, Hansson H, Kim S, Piens K, Mitchinson C and Sandgren M (2008) The first structure of a glycoside hydrolase family 61 member, Cel61B from *Hypocrea jecorina*, at 1.6 Å resolution. J Mol Biol 383:144–154. https://doi.org/10.1016/j.jmb.2008.08.016

Kobayashi K, Sumitomo H, Ina Y (1985) Synthesis and functions of polystyrene derivatives having pendant oligosaccharides. Polym J 17:567–575. https://doi.org/10.1295/polymj.17.567

Kobayashi K, Kamiya S, Enomoto N (1996) Amylose-carrying styrene macromonomer and its homo- and copolymers: synthesis via enzyme-catalyzed polymerization and complex formation with iodine. Macromolecules 29(27):8670-8676. http://doi.org/10.1021/ma9603443

Kracher D, Scheiblbrandner S, Felice AK, Breslmayr E, Preims M, Ludwicka K, Haltrich D, Eijsink VG, Ludwig R (2016) Extracellular electron transfer systems fuel cellulose oxidative degradation. Science 352:1098-1101. http://doi.org/10.1126/science.aaf3165

Langsford ML, Gilkes NR, Singh B, Moser B, Miller RC Jr, Warren RA, Kilburn DG (1987) Glycosylation of bacterial cellulases prevents proteolytic cleavage between functional domains. FEBS Lett 225(1-2):163-7. http://doi.org/10.1016/0014-5793(87)81150-x

Levasseur A, Drula E, Lombard V, Coutinho PM, Henrissat B (2013) Expansion of the enzymatic repertoire of the CAZy database to integrate auxiliary redox enzymes. Biotechnol Biofuels 6:41. https://doi.org/10.1186/1754-6834-6-41

Levasseur A, Lomascolo A, Chabrol O, Ruiz-Dueñas FJ, Boukhris-Uzan E, Piumi F, Kües U, Ram AF, Murat C, Haon M, Benoit I, Arfi Y, Chevret D, Drula E, Kwon MJ, Gouret P, Lesage-Meessen L, Lombard V, Mariette J, Noirot C, Park J, Patyshakuliyeva A, Sigoillot JC, Wiebenga A, Wösten HA, Martin F, Coutinho PM, de Vries RP, Martínez AT, Klopp C, Pontarotti P, Henrissat B, Record E (2014) The genome of the white-rot fungus *Pycnoporus cinnabarinus*: a basidiomycete model with a versatile arsenal for lignocellulosic biomass breakdown. BMC Genomics 15:486. http://doi.org/10.1186/1471-2164-15-486

Levin L, Villalba L, Da Re V, Forchiassin F, Papinutti L (2007) Comparative studies of loblolly pine biodegradation and enzyme production by Argentinean white rot fungi focused on biopulping processes. Process Biochem 42:995–1002. https://doi.org/10.1016/j.procbio.2007.03.008

Li X, Beeson WT, Phillips CM, Marletta MS, Cate JHD (2012) Structural basis for substrate targeting and catalysis by fungal polysaccharide monooxygenases. Structure 20:1051–1061. http://doi.org/10.1016/j.str.2012.04.002

Linder S, Schliwa M, Kube-Granderath E (1996) Direct PCR screening of *Pichia pastoris* clones. Biotechniques 20:980-982. https://doi.org/10.2144/96206bm08

Liu B, Olson Å, Wu M, Broberg A, Sandgren M (2017) Biochemical studies of two lytic polysaccharide monooxygenases from the white-rot fungus *Heterobasidion irregulare* and their roles in lignocellulose degradation. PLoS One 12(12). http://doi.org/10.1371/journal.pone.0189479

Liu B, Kognole AA, Wu M, Westereng B, Crowley MF, Kim S, Dimarogona M, Payne CM, Sandgren M (2018) Structural and molecular dynamics studies of a C1-oxidizing lytic polysaccharide monooxygenase from *Heterobasidion irregulare* reveal amino acids important for substrate recognition. FEBS Journal 285:2225–2242. http://doi.org/10.1111/febs.14472

Lomascolo A, Uzan-Boukhris E, Herpoël-Gimbert I, Sigoillot JC, Lesage-Meessen L (2011) Peculiarities of *Pycnoporus* species for applications in biotechnology. Appl Microbiol Biotechnol 92:1129–1149. https://doi.org/10.1007/s00253-011-3596-5

Lundell TK, Mäkelä MR, Hildén K (2010) Lignin-modifying enzymes in filamentous basidiomycetes - ecological, functional and phylogenetic review. J Basic Microbiol 50(1): 5–20. http://doi.org/10.1002/jobm.200900338

Mhlongo SI, den Haan R, Viljoen-Bloom M, van Zyl WH (2015) Lignocellulosic hydrolysate inhibitors selectively inhibit/deactivate cellulase performance. Enzyme Microb Tech 81:16–22. http://doi.org/10.1016/j.enzmictec.2015.07.005

Miyauchi S, Navarro D, Grigoriev IV, Lipzen A, Riley R, Chevret D,Grisel S, Berrin J-G, Henrissat B, Rosso M-N (2016) Visual comparative omics of fungi for plant biomass deconstruction. Front Microbiol 7:1335. https://doi.org/10.3389/fmicb.2016.01335

Miyauchi S, Navarro D, Grisel S, Chevret D, Berrin J-G, Rosso M-N (2017) The integrative omics of white-rot fungus *Pycnoporus coccineus* reveals co-regulated CAZymes for orchestrated lignocellulose breakdown. PLoS ONE 12(4):e0175528. https://doi.org/10.1371/journal. pone.0175528

Moses V, Hatherley R, Bishop OT (2016) Bioinformatic characterization of type-specifc sequence and structural features in auxiliary activity family 9 proteins. Biotechnol Biofuels 9:239. http://doi.org/10.1186/s13068-016-0655-2

Müller G, Várnai A, Salomon Johansen K, Eijsink VGH and Horn SJ (2015) Harnessing the potential of LPMO-containing cellulase cocktails poses new demands on processing conditions. Biotechnol Biofuels 8:187. http://doi.org/10.1186/s13068-015-0376-y

Niderhaus N, Garrido M, Insani M, Campos E, Wirth SA (2018) Heterologous production and characterization of a thermostable GH10 family endo-xylanase from *Pycnoporus sanguineus* BAFC 2126. Proc Bio 67:92–98. https://doi.org/10.1016/j.procbio.2018.01.017

Quinlan RJ, Sweeney MD, Lo Leggio L, Otten H, Poulsen JC, Johansen KS, Krogh KB, Jørgensen CI, Tovborg M, Anthonsen A, Tryfona T, Walter CP, Dupree P, Xu F, Davies GJ, Walton PH (2011) Insights into the oxidative degradation of cellulose by a copper metalloenzyme that exploits biomass components. Proc Natl Acad Sci USA108(37):15079-84. http://doi.org/10.1073/pnas.1105776108

Robert X, Gouet P (2014) Deciphering key features in protein structures with the new ENDscript server. Nucleic Acids Res 42:W320-W324. http://doi.org/10.1093/nar/gku316

Rohr CO, Levin LN, Mentaberry AN, Wirth SA (2013) A first insight into *Pycnoporus sanguineus* BAFC 2126 transcriptome. PLoS One 8(12):e81033. http://doi.org/10.1371/journal.pone.0081033

Rooijakkers BJM, Ikonen MS, Linder MB (2018) Fungal-type carbohydrate binding modules from the coccolithophore *Emiliania huxleyi* show binding affinity to cellulose and chitin. PLoS One 13(5):e0197875. http://doi.org/10.1371/journal.pone.0197875

Sabbadin F, Hemsworth GR, Ciano L, Henrissat B, Dupree P, Tryfona T, Marques R, Sweeney ST, Besser K, Elias L, Pesante G, Li Y, Dowle AA, Bates R, Gomez LD, Simister R, Davies GJ, Walton PH, Bruce NC, McQueen-Mason SJ (2018) An ancient family of lytic polysaccharide monooxygenases with roles in arthropod development and biomass digestion. Nat Commun 9:756. https://doi.org/10.1038/s41467-018-03142-x

Tamura K, Stecher G, Peterson D, Filipski A, and Kumar S (2013) MEGA6: molecular evolutionary genetics analysis version 6.0. Mol Biol Evol 30:2725-2729. http://doi.org./10.1093/molbev/mst197

Vaaje-Kolstad G, Westereng B, Horn SJ, Liu Z, Zhai H, Sørlie M, Eijsink VG (2010) An oxidative enzyme boosting the enzymatic conversion of recalcitrant polysaccharides. Science 30(6001):219-22. http://doi.org/10.1126/science.1192231

Vaaje-Kolstad G, Forsberg Z, Loose JSM, Bissaro B and Eijsink VGH (2017) Structural diversity of lytic polysaccharide monooxygenases. Curr Opin Struc Biol 44:67–76. http://dx.doi.org/10.1016/j.sbi.2016.12.012

Vaaje-Kolstad G, Tuveng TR, Mekasha S, and Eijsink, VGH (2019) Enzymes for modification of chitin and chitosan. In: L.A. Broek and C.G. Boeriu (eds) Chitin and chitosan: properties and applications, Wiley, New York, pp 189-228. http://doi.org/10.1002/9781119450467.ch8

Várnai A, Mäkelä MR, Djajadi DT, Rahikainen J, Hatakka A, Viikari L (2014) Carbohydrate-binding modules of fungal cellulases: occurrence in nature, function, and relevance in industrial biomass conversion. Adv Appl Microbiol 88:103-165. http://doi.org/10.1016/B978-0-12-800260-5.00004-8

Zhang J, Silverstein KAT, Castaño JD, Figueroa M, Schilling JS (2019) Gene regulation shifts shed light on fungal adaption in plant biomass decomposers. MBio 10:e02176-19. https://doi.org/10.1128/mBio.02176-19

FIGURE LEGENDS

Fig. 1 In silico analysis of *Ps*AA9A. Three-dimensional structure of *Ps*AA9A catalytic module. The catalytic residues His 1, His 80 and Tyr 167 are highlighted in violet and the copper atom is shown as a green sphere. Tyrosine residues 20 and 36, located in the substrate binding surface, are highlighted in orange. This image was made with VMD software support. VMD is developed with NIH support by the Theoretical and Computational Biophysics group at the Beckman Institute, University of Illinois at Urbana-Champaign **(A)**. Phylogenetic tree constructed using Neighbor Joining statistical method. The optimal tree is drawn to scale and the percentage of replicate trees in which the associated sequences clustered together in the boostrap test (1000 replicates) are shown next to the branches. *Ps*AA9A is highlighted in blue.

NCBI GenBank accession numbers for each sequence are indicated between parenthesis **(B)**. Phylogenetic and molecular evolutionary analyses were conducted using MEGA version 6 (Tamura et al. 2013)

Fig. 2 HPAEC-PAD and MALDI-TOF analysis of the glucan products after treating PASC with *Ps*AA9A. HPAEC-PAD overlapped chromatograms of products obtained after incubation of 0.5% PASC with (blue) and without (black) 2 µM *Ps*AA9A and 1 mM ascorbic acid for 24 h **(A)**. MALDI-TOF spectra of products obtained under the same reaction conditions **(B)**. Glc_n stands for native cello-oligosaccharides and Glc_n-GlcA represents C1 oxidized aldonic sugars. The main peaks correspond to mono- or di- sodiated adducts of C1 aldonic acids, imparting +16 and +38 units respectively, relative to the mono-sodiated unoxidized form. DP: degree of polymerization; a.u.: arbitrary unit. HPAEC-PAD standards: Identity of Glc_n was assigned by commercial standards, Gcl-GclA by an in-house standard, and $Glc_{(2-5)}$-GlcA were inferred from retention times of previous references

Fig. 3 MALDI-TOF analysis of the glucan products after treating Avicel and β-chitin with *Ps*AA9A. MALDI-TOF spectra in positive ion mode showing native and oxidized oligosaccharides obtained after incubation of 0.4% avicel **(A)** and β-chitin **(B)** with 2 µM *Ps*AA9A and 4 mM ascorbic acid for 24 h. Incubation of 0.4% avicel and β-chitin with 2 µM *Ps*AA9A in the absence of the electron donor are shown in **(C)** and **(D)**, respectively. For both substrates, the main signals correspond to native oligosaccharides and mono- or di- sodiated adducts of C1 aldonic acids, imparting +16 and +38 units respectively, relative to the mono-sodiated unoxidized form. Smaller signals for the mono-sodiated lactone (-2 units from the unoxidized form) were also identified. DP: degree of polymerization; a.u.: arbitrary unit

Fig. 4 Combined activity of *Ps*AA9A with commercial GHs. Quantification by HPAEC-PAD analysis, showing the release of glucose by a commercial GH1 **(A)** and cellobiose by commercial GH5 **(B),** GH6 **(C)**, and GH7 **(D)** from 0.4% PASC over 3h at 30°C, in presence (+) or absence (-) of *Ps*AA9A and/or gallic acid. SI stands for Synergism Index, calculated as the glucan release by GH + *Ps*AA9A + gallic acid (black bar)/ glucan release by GH + gallic acid (white bar). Bars indicate means (error bars: standard deviations of three replicates). The identity and quantity of each species was determined by analysis of commercial standards. Tukey test was performed to determine significant differences between means (asterisks)

*Ps*AA9A, a C1-specific AA9 lytic polysaccharide monooxygenase from the white-rot basidiomycete *Pycnoporus sanguineus*

Mercedes María Garrido[1,2], Malena Landoni[3], Federico Sabbadin[4], María Pía Valacco[5], Alicia Couto[3], Neil Charles Bruce[4], Sonia Alejandra Wirth[2], Eleonora Campos[1]

1- Instituto de Agrobiotecnología y Biología Molecular (IABIMO), Instituto Nacional de Tecnología Agropecuaria (INTA-CONICET). Los Reseros y Nicolas Repetto s/n (1686), Hurlingham, Buenos Aires, Argentina.
2- Laboratorio de Agrobiotecnología, Instituto de Biodiversidad y Biología Experimental y Aplicada (IBBEA) CONICET-UBA, Facultad de Ciencias Exactas y Naturales, Universidad de Buenos Aires (C1428EG), Buenos Aires, Argentina.
3- Centro de Investigación en Hidratos de Carbono (CIHIDECAR), Facultad de Ciencias Exactas y Naturales, Universidad de Buenos Aires (C1428EG), Buenos Aires, Argentina.
4- Centre for Novel Agricultural Products (CNAP), Department of Biology, University of York, York YO10 5DD, UK.
5- Instituto de Química Biológica (IQUIBICEN), Facultad de Ciencias Exactas Y Naturales, Universidad de Buenos Aires (C1428EG), Buenos Aires, Argentina.

Corresponding author: Eleonora Campos (campos.eleonora@inta.gob.ar)
Other authors: garrido.mercedes@inta.gob.ar; mlandoni@qo.fcen.uba.ar; federico.sabbadin@york.ac.uk; pvalacco@qb.fcen.uba.ar; acouto@qo.fcen.uba.ar; neil.bruce@york.ac.uk; sonia.wirth@gmail.com

KEY WORDS
Pycnoporus; LPMO; AA9; CELLULOSE

ABSTRACT
Woody biomass represents an important source of carbon on earth and its global recycling is highly dependent on *Agaricomycetes* fungi. White-rot *basidiomycetes* are a very important group in this regard, as they possess a large and diverse enzymatic repertoire for biomass decomposition. Among these enzymes, the recently discovered lytic polysaccharide monooxygenases (LPMOs) have revolutionized biomass processing with their novel oxidative mechanism of action. The strikingly high representation of LPMOs in fungal genomes raises the question of their functional versatility. In this work, we studied an AA9 LPMO from the white-rot basidiomycete *Pycnoporus sanguineus*, *Ps*AA9A. Successfully produced as a recombinant secreted protein in *Pichia pastoris*, *Ps*AA9A was found to be a C1-specific LPMO active on cellulosic substrates, generating native and oxidized cello-oligosaccharides in the presence of an external electron donor. *Ps*AA9A boosted cellulolytic activity of glysoside hydrolases from families GH1, GH5, and GH6.This study serves as a starting point towards understanding the functional versatility and biotechnological potential of this enzymatic family, highly represented in wood decay fungi, in *Pycnoporus* genus.

KEY POINTS
*Ps*AA9A is the first AA9 from *P. sanguineus* to be characterized.
*Ps*AA9A has activity on cellulose, producing C1-oxidized cello-oligosaccharides.
Boosting activity with GH1, GH5 and GH6 was proven.

INTRODUCTION

Agaricomycetes fungi are the major decomposers of organic matter and dominate the recycling of its sequestered carbon. Within this class of *basidiomycetes*, wood-decaying fungi follow different strategies for lignocellulose decomposition using a diverse plethora of hydrolytic and oxidative enzymes as well as non-enzymatic processes. The most representative order of *Agaricomycetes* causing wood decay is the *Polyporales,* which includes the genus *Pycnoporus* with four worldwide distributed species that cause wood decay by white rot, meaning that they are able to efficiently mineralize the lignin of plant cell walls (Lundell et al. 2010). *Pycnoporus* species have been recognized for their biotechnological potential because they synthesize high value-added compounds (Falconnier et al. 1994; Asther et al. 1998; Alvarado et al. 2003) and carbohydrate active enzymes with remarkable thermal stability and broad pH range activity

(Lomascolo et al. 2011; Falkoski et al. 2012; Niderhaus et al. 2018). In addition, the high efficiency of *Pyncoporus* species for the decomposition of hard and soft wood has generated a growing interest in the study of the enzymes involved and the correlating mechanisms (Levin et al. 2007; Levasseur et al. 2014; Couturier et al. 2015). Comparative transcriptomic and secretomic analysis of *Pyncoporus sanguineus* grown in complex plant materials allowed the identification of differentially expressed genes and the corresponding secreted proteins (Miyauchi et al. 2016). In subsequent work, the same authors compared the transcriptomic and secretomic expression patterns at different time points in response to different lignocellulosic substrates of *Pyncoporus coccineus*, a very closely related fungus. The study concluded that genes encoding enzymes associated with a Carbohydrate Binding Module (CBM1) were strongly up-regulated and that there was a close involvement of AA9 lytic polysaccharide monooxigenases (LPMOs) in adaptive responses of the fungi to complex substrates (Miyauchi et al. 2017). Of the 16 AA9 LPMOs identified in *P. sanguineus* genome, none have been characterized to date.

LPMOs are metalloenzymes that bind a copper atom through a characteristic and highly conserved histidine brace (Quinlan et al. 2011). An external electron donor reduces the copper provoking a reaction between the enzyme with either O_2 or H_2O_2 and consequently a powerful oxygen species is created which can then oxidize and break the glycosidic bond either at the C1 or C4 position (Eijsink et al. 2019). LPMOs are currently classified by CAZY as Auxilliary Active Enzymes (AA) (Levasseur et al. 2013) and, to date, make up seven different families (AA9, AA10, AA11, AA13, AA14, AA15 and AA16) based on sequence similarity. Interestingly, the active site is typically positioned on a flat surface (Karkehabadi et al. 2008) which enables the enzyme to oxidize crystalline polysaccharides (Aachmann et al. 2012), making them more accessible to glycoside hydrolases (GHs) and playing a crucial role in polysaccharide degradation (Harris et al. 2010; Vaaje-Kolstad et al. 2010; Muller et al. 2015). Cellulose-active AA9 LPMOs show different regioselectivities producing either C1-oxidized products (lactones, that spontaneously convert to aldonic acids), C4-oxidized products (ketones, that spontaneously convert to gemdioles), or a mixture of both (Vaaje-Kolstad et al. 2017). In recent years, a lot of effort has been dedicated into finding phylogenetic relationships between regioselectivity, substrate specificity and amino acid sequence of AA9 LPMOs (Li et al. 2012; Moses et al. 2016) but no determinant feature has been identified yet (Frommhagen et al. 2018). The diversity of AA9s in white-rot fungi is thought to allow wider substrate specificity and biochemical adaptability (Berrin et al. 2017).

The *P. sanguineus* genome was made publicly available in 2014 by the Joint Genome Institute (JGI, Department of Energy, USA) and several transcriptomic and secretomic studies have been carried out on this species and closely related ones (Rohr et al. 2013; Miyauchi et al. 2016; 2017; Zhang et al. 2019). Among 16 putative AA9 LPMOs encoded in *P. sanguineus* genome, this work focuses on *Ps*AA9A. The transcript for *Ps*AA9A (JGI, *P. sanguineus* BRFM 1264 v1.0, transcript ID: 1583829) was the most strongly upregulated in lignocellulose-containing media (Miyauchi et al. 2016) and the only LPMO sequence featuring an appended CBM. Also, the gene encoding *Ps*AA9A has been found to be differentially expressed when *P. sanguineus* was grown in wheat straw as opposed to its growth in maltose. Additionally, it was found to be co-regulated with genes coding for a GH131_CBM1, CBM1_GH6, CBM1_GH5_7, AA8-AA3_1, GH7, GH74, and GH28 (Miyauchi et al. 2016) which suggested that these proteins may act in synergy to degrade this complex substrate.

We present here the first functional characterization of *Ps*AA9A including its regioselectivity, activity in the presence of various electron donors, synergism with canonical GHs and substrate specificity. This study sheds the first light on the biological basis of AA9 multiplicity in this major white-rot genus, and opens up new opportunities for its biotechnological exploitation.

MATERIALS AND METHODS

Cloning of *Ps*AA9A

The full coding sequence for *Ps*AA9A (protein ID: 1583489, JGI) from *P. sanguineus,* including its native signal sequence and without stop codon, was obtained from *P. sanguineus* genome publicly available at Joint Genome Institute portal (https://mycocosm.jgi.doe.gov/Pycsa1/Pycsa1.home.html) and was synthesized for expression in *P. pastoris* using the gene synthesis and codon optimization service by Genescript (Piscataway, USA) (supplied in pUC57 plasmid, cloned in *Eco*RV restriction site). Synthetic

DNA sequence was deposited at GenBank under accession number MT076044. For expression of mature *Ps*AA9A fused to a C-terminal 6xHIS tag in *P. pastoris*, the *Bam*HI/*Spe*I restriction product was cloned into the pPICHIS vector, a derivative of pPIC9 (Invitrogen Life Technologies, Waltham, USA), replacing the α-factor signal sequence to obtain plasmid p*Ps*AA9AHis. Plasmid pPICHIS contains a 6-histidine coding sequence in frame with *Spe*I and followed by a stop codon (Campos et al. 2016).

Prediction of signal peptide and processing site in the translated protein was performed using SignalP 4.0 software (http://www.cbs.dtu.dk/services/SignalP/) and prediction of *N*- and *O*-glycosylation sites with NetNGlyc 1.0 Server (http://www.cbs.dtu.dk/services/NetNGlyc/) and NetOGlyc 4.0 Server (http://www.cbs.dtu.dk/services/NetOGlyc/), respectively.

Recombinant *Ps*AA9A expression in *P. pastoris* and purification

Recombinant vector p*Ps*AA9AHis was linearized with *Bgl*II restriction enzyme and used for transformation of *P. pastoris* strain GS115 (Invitrogen Life Technologies, Waltham, USA) by electroporation. Recombinant clones reverting histidine auxotrophy were selected on minimal medium MD plates (0.34% yeast nitrogen base without amino acids, 10 g/L $(NH_4)_2SO_4$, 2% dextrose and 2% agar). Integration in the AOX1 locus of the *P. pastoris* genome was verified by colony PCR using the universal primers 5'AOX1 (GACTGGTTCCAATTGACAAGC) and 3'AOX1 (GCAAATGGCATTCTGACATCC) (Linder et al. 1996). Single colonies were suspended in 100 µL sterile water and incubated with 15 U of Lyticase from *Arthrobacter luteus* (Sigma Aldrich, Saint Louis, USA) for 30 min at 37°C, boiled for 5 min and the DNA was recovered by centrifugation at 12000 g for 5 min. PCR amplifications were performed in 50 µL volumes reaction with 15 µL of DNA template, 50 pmol of each primer, 0.2 mM of each dNTP, 2 mM $MgCl_2$, 1 unit of Taq polymerase and 1X reaction buffer (Invitrogen Life Technologies, Waltham, USA). After an initial denaturation of 3 min at 95°C, the amplification was carried out for 30 cycles of 95°C, 30 sec; 60°C, 30 sec and 72°C, 2.5 min and a final single step of 72°C, 10 min. Positive clones were selected and conserved on MD or YPD (1% yeast extract, 2% peptone, 2% dextrose, 2% agar) agar slants.

Histidine tagged recombinant protein production in *P. pastoris* and purification by Ni-NTA affinity chromatography was performed in the same conditions as previously described (Campos et al. 2016). Briefly, pre-inoculums were generated in 5 mL of YPD medium and 1 mL was used as seed to inoculate 80 mL of BMGY (1% yeast extract, 2% peptone, 0.34% yeast nitrogen base without amino acids, 10 g/L $(NH_4)_2SO_4$, 400 mg/L biotin, 4% glycerol, 100 mM potassium phosphate buffer, pH 6.0) in 500 mL shake flasks and cultivated for 48 h at 30°C and 220 rpm. Cells were harvested by centrifugation 5 min at 1500 g and resuspended in 300 mL of BMMY medium (1% yeast extract, 2% peptone, 100 mM potassium phosphate buffer, pH 6.0, 0.34% yeast nitrogen base without amino acids, 10 g/L $(NH_4)_2SO_4$, 400 mg/L biotin) to a final OD600 nm = 2.5 and cultivated in 1 L shake flasks at 28°C and 220 rpm. Sterile methanol (0.5% final) was added every 24 h to maintain induction conditions.

P. pastoris cultures were harvested after 4 days of induction and centrifuged at 1500 g for 10 min. The supernatant was concentrated by ultrafiltration (30 kDa MWCO, Amicon Ultra. Merck Millipore, Burlington, USA) and buffer exchanged to equilibration buffer (300 mM NaCl, 50 mM sodium phosphate buffer, pH 8). Recombinant *Ps*AA9A was purified by gravity flow Ni-NTA affinity chromatography using His select nickel affinity gel (Sigma Chemical Co., Saint Louis, USA). In order to saturate the active site with copper, 5-fold molar excess of a 20 mM $CuSO_4$ solution was decanted into the protein solution while mixing gently to avoid precipitation and then loaded into a HiLoad 16/60 Superdex 75 prep grade column (GE Healthcare, Chicago, USA) for size exclusion chromatography, to remove salts and unbound copper. The purified protein was eluted from the column in 20 mM sodium phosphate buffer pH 7. The resulting yield was 7.5 mg of purified copper-saturated protein obtained from a 1 L culture.

Polyacrylamide gel electrophoresis and immunoblotting

Recombinant *Ps*AA9A in crude cell-free extracts was separated by reducing 12% SDS-PAGE and identified by Coomassie Blue staining or transferred to 0.45 µm nitrocellulose membrane (Bio-Rad Laboratories Inc, Hercules, USA). Western blot was performed by probing the membrane with 0.1 µg/mL of polyclonal rabbit anti-HIS antibody (Genescript, Piscataway, USA) followed by 1:15000 dilution of alkaline phosphatase-linked goat anti-rabbit antibody (Sigma Chemical Co., Saint Louis, USA). Phosphatase activity was revealed by a chromogenic reaction using 5-bromo-4-chloro-3-indolyl phosphate (BCIP) and nitroblue tetrazolium (NBT) as substrates (Sigma Chemical Co., Saint Louis, USA).

Thermal shift assay (Thermofluor)

SyPro orange protein gel stain (Invitrogen Life technologies S6650, Waltham, USA) reactant was added to 5 µM *Ps*AA9A alone or in the presence of 10 mM EDTA and thermofluor assay was conducted using an Mx3005P qPCR System (Agilent Technologies, Santa Clara, USA). The intensity of the fluorescence was measured at a temperature gradient (25°C - 90°C with 1°C intervals) and converted into a melting curve to determine the melting temperature (Tm).

Proteomic analysis

Purified *Ps*AA9A was quantified by Bradford assay (Promega, Biodynamics, CABA, Argentina), then precipitated with 10% trichloro acetic acid (TCA) and resuspended in water (18 Ω) to a final concentration of 1 mg/mL. Protein digestion and mass spectrometry analysis were performed at CEQUIBIEM (http://cequibiem.qb.fcen.uba.ar/). The protein sample was reduced with dithiotreitol 10 mmol/L for 45 min at 56 °C, alkylated with iodo acetamide (55 mmol/L) for 45 min in the dark and digested with trypsin (Promega V5111; Promega, Fitchburg, WI) overnight at 37°C. The digests were analyzed by nano LC-MS/MS in a Thermo Scientific Q-Exactive Mass Spectrometer coupled with a nano HPLC EASY-nLC 1000 (Thermo Fisher Scientific, CABA, Argentina). For the LC-MS/MS analysis, approximately 1 µg of peptides was loaded onto the column and eluted for 120 min using a reverse phase column (C18, 2 lm, 100 A, 50 lm 9 150 mm) Easy-Spray Column PepMap RSLC (P/N ES801) suitable for separating complex peptide mixtures with a high degree of resolution. The flow rate used for the nano column was 300 nL/min and the solvent range from 7% B (5 min) to 35% (120 min). Solvent A was 0.1% formic acid in water, whereas B was 0.1% formic acid in acetonitrile. The injection volume was 2 µL. A voltage of 3.5 kV was used for Electro Spray Ionization (Thermo Fisher Scientific; EASYSPRAY, Thermo Fisher Scientific, CABA, Argentina). The MS equipment has a high collision dissociation cell (HCD) for fragmentation and an Orbitrap analyser (Thermo Fisher Scientific; Q-Exactive, Thermo Fisher Scientific, CABA, Argentina). XCALIBUR3.0.63 (Thermo Fisher Scientific, Thermo Fisher Scientific, CABA, Argentina) software was used for data acquisition and equipment configuration to allow simultaneous chromatographic separation and peptide identification. Full-scan mass spectra were acquired in the Orbitrap analyser. The scanned mass range was 400–2,000 m/z, at a resolution of 70,000 at 400 m/z, and the 12 most intense ions in each cycle, were sequentially isolated, fragmented by HCD and measured in the Orbitrap analyser. Peptides with a charge of +1 or with unassigned charge state were excluded from fragmentation for MS2. Q Exactive raw data was processed using Proteome Discoverer software (version 2.1.1.21 Thermo Scientific, Thermo Fisher Scientific, CABA, Argentina) and searched against the expected sequences, with trypsin specificity and a maximum of one missed cleavage per peptide. Carbamidomethylation of cysteine residues was set as a fixed modification and oxidation of methionine was set as variable modification, a precursor mass tolerance of 10 ppm and product ion tolerance to 0.05 Da. No-enzyme searches were also performed to analyze the N-terminal portion of the protein.

In vitro activity assays

Typical reactions for *Ps*AA9A characterization were carried out by mixing 1-5 mg/mL PASC with 1-2 µM purified protein, 1-4 mM electron donor (ascorbic or gallic acid), in a total volume of 100 µL in 2 mL plastic reaction tubes. The other substrates (avicel, β-chitin, pachyman, glucomannan, galactomannan, lichenan, xyloglucan, xylan from beechwood, and α-chitin) and electron donors (pyrogallol, caffeic acid, ferulic acid and *p*-coumaric acid) tested were used in the same conditions. All reactions analyzed via MALDI-TOF were carried out in 50 mM ammonium acetate buffer pH 6 and incubated at 30°C shaking at 600 rpm and the supernatant used for analysis.

Reactions used for product quantification and synergism experiments with *Ps*AA9A were typically carried out in 50 mM sodium phosphate buffer pH 6 in triplicates of 100 µL each for 3 h at 30°C at 600 rpm. Each reaction contained 2 µM purified *Ps*AA9A, 1–4 mg/mL PASC, and 1 mM gallic acid. Commercial GH1 (4 mU; cat. Number E-BGOSAG, Megazyme, Bray, Ireland), GH5 (6 mU; cat. number E-CELBA, Megazyme, Bray, Ireland), GH6 (0.8 mU; cat. number E-CBHIIM, Megazyme, Bray, Ireland), and GH7 (0.1 mU; cat. number E-CBHI, Megazyme, Bray, Ireland) were added to 100 µL reactions. After 3 h incubation, 400 µL of ethanol were added to stop the reaction, spun down and 400 µL of supernatant was transferred

to new plastic tubes, dried down and re-suspended in 160 µL of pure water, filtered and analyzed via HPAEC-PAD.

In all cases, controls of substrate with and without electron donor (without enzyme) and substrate with enzyme (without electron donor) were included in the analysis.

Product analysis by HPAEC-PAD

Oligosaccharides were analyzed via High-performance Anion Exchange Chromatography (HPAEC) using a ICS-3000 Pulsed Amperometric Detection (PAD) system with an electrochemical gold electrode, a CarboPac PA20 3 × 150 mm analytical column and a CarboPac PA203 × 30 mm guard column (Dionex, Thermo Fisher Scientific, CABA, Argentina). Sample aliquots of 5 µL were injected and separated at a flow rate of 0.5 mL/min at a constant temperature of 30 °C. After equilibration of the column with 50% H_2O-50% 0.2 M NaOH, a 30-min linear gradient was started from 0% to 20% with 0.5 M sodium acetate in 0.2 M NaOH and then kept constant for 20 min. The column was then washed with 0.2 M NaOH for 6 min and re-equilibrated for 4 min with 50% H_2O-50% 0.2 M NaOH before starting the next run (oligosaccharide method).

Glucose was analyzed with the following HPAEC program (monosaccharide method). After equilibration of the column with 100% H_2O, sample aliquots of 5 µL were injected and separated at a flow rate of 0.5 mL/min at a constant temperature of 25 °C. The column was washed with 100% H_2O for 10 min, followed by 9 min of 99% H_2O-1% 0.2 M NaOH. The column was then washed with 0.2 M NaOH for 6 min and re-equilibrated with 100% H_2O before injection of the next sample. Integrated peak areas were compared to mono and oligo-saccharide calibration standards (glucose, cellobiose, cellotriose, cellotetraose, cellopentaose, cellohexaose, *N*-acetylglucosamine, chitobiose, chitotriose, chitotetraose, chitopentaose) purchased from Megazyme (Bray, Ireland). C1 oxidized cellobiose standard was chemically synthesized as described in the following section.

Synthesis of C1 oxidized cellobiose standard

The cellobiose was chemically oxidized as previously described (Forsberg et al. 2011) using a mild oxidation method that has been shown to selectively oxidize the hemiacetal carbon of carbohydrates to generate aldonic acids (Kobayashi et al. 1985 and 1996). Briefly, the cellobiose (0.2 g) was dissolved in 2 mL water and mixed with an iodine solution (7.3 mmol iodine in 15 mL methanol). While stirring, 5 mL of a 4% (w/w) solution of KOH in methanol was added dropwise for 5 min and then the reaction was kept at room temperature for 30 min. The solution was heated to 40°C for 1 h until the color disappeared. Cooling in the refrigerator overnight yielded a precipitate of white crystals that was filtered and washed with cold methanol. The solid was redissolved in 2 mL water. The product was analyzed by HPAEC-PAD in the same conditions described above.

Product analysis by mass spectrometry

One microliter of reaction supernatant was mixed with an equal volume of 20 mg/mL 2,5-dihydroxybenzoic acid (DHB) in 50% acetonitrile, 0.1% TFA on a SCOUT-MTP 384 target plate (Bruker, Billerica, USA). The spotted samples were then dried in a vacuum desiccator before being analyzed by mass spectrometry on an Ultraflex III matrix-assisted laser desorption ionization time of flight/time of flight (MALDI/TOF-TOF) instrument (Bruker, Billerica, USA) (Abdul Rahman et al. 2014).

RESULTS

In silico and phylogenetic analysis of *Ps*AA9A

In silico analysis of *Ps*AA9A showed the presence of an N-terminal signal peptide for secretion, and conserved residues (His 1, His 80, Tyr 167, of the mature protein) involved in copper coordination within the catalytic site (Fig. 1a). A CBM1, containing four conserved cysteine residues involved in disulfide bridge formation and the conserved aromatic residues (Y4, Y30 and Y31) involved in ligand recognition (Gilkes et al. 1991, Varnai et al. 2014), is located at C-terminus linked to the catalytic domain by a flexible linker rich in proline-threonine residues. Phylogenetic analysis of the mature catalytic domain of *Ps*AA9A and other biochemically characterized AA9 LPMOs placed *Ps*AA9A in a cluster together with *Hi*LPMOB

(GenBank ETW87087.1) and *Mt*PMO3 (GenBank AEO56665.1), both C1-specific AA9 LPMOs from the white-rot basidiomycete *Heterobasidion irregulare* and the ascomycete *Myceliophthora thermophila* respectively (Fig. 1b). Alignment of *Ps*AA9A with *Hi*LPMOB and *Mt*PMO3 revealed that *Ps*AA9A has several features that were shown to be present in *Hi*LPMOB and *Mt*PMO3 but not in other C1-specific LPMOs (Supplemental Fig. S1). These three enzymes have a longer L2 loop (10-aminoacid extension) with an aromatic residue in position 20 and a Tyr residue (Tyr36 in *Ps*AA9A) that were found to be located on the substrate binding surface in the vicinity of the active-site copper (Liu et al. 2018) (Fig. 1a). Moreover, they have a shorter L3 loop devoid of a conserved Tyr residue, replaced by Pro79 in *Ps*AA9A and *Hi*LPMOB, and Tre74 in *Mt*PMO3.

Recombinant *Ps*AA9A produced in *P. pastoris*

*Ps*AA9A was successfully produced from *P. pastoris* transformants and secreted to the extracellular media with an apparent molecular mass higher than the theoretical one (55 and 31.27 KDa, respectively) (Supplemental Fig. S2), which could be explained by the presence of a potential *N*-glycosylation site at position 134 of the mature protein and to *O*-glycosylation in the serine/threonine rich linker region between the catalytic module and the CBM1 (Langsford et al. 1987; Abuja et al. 1988). Mass spectrometry analysis revealed the presence of correctly processed mature protein containing the N-terminal His catalytic residue. However, peptides retaining three additional amino acids from the signal peptide in the N-terminal portion of the protein were also detected. This can be related to random incorrect processing of foreign signal peptides, which has also been recently reported for other recombinant LPMOs expressed in *P. pastoris* (Jagadeeswaran et al. 2018; Eijsink et al. 2019).

Thermal shift analysis of the *Ps*AA9A copper-saturated protein indicated a melting temperature (Tm) of 47.9°C, which decreased to 46.3°C upon addition of 10 mM EDTA, indicating that copper binding to the active site increased protein thermal stability, as previously observed for other LPMOs such as *Td*AA15A (Sabbadin et al. 2018) (Supplemental Fig. S3).

***Ps*AA9A acts with C1-oxidative regioselectivity**

Based on the fact that AA9 LPMOs characterized to date are mainly known for being active on crystalline cellulose and that the protein in study is fused to a CBM1 module (which usually binds cellulose), we first evaluated the activity and regioselectivity of *Ps*AA9A on Phosphoric Acid Swollen Cellulose (PASC), using ascorbic acid as electron donor. After 24 hours of incubation, soluble reaction products were analyzed by mass spectrometry (MALDI-TOF) and HPAEC-PAD revealing peaks corresponding to native and C1-oxidized cello-oligosaccharides (COS) with degrees of polymerization (DP) 2 to 5 (Fig. 2). Commercial native COS and in-house chemically synthesized C1-oxidized cellobiose were used as standards for HPAEC-PAD analysis. Similar reactions were carried out at different temperatures (30, 40, 45, 50 and 60 °C) and pH (5, 5.5, 6 and 7.5) releasing native and oxidized COS in all the conditions tested, demonstrating the versatility of the enzyme. (Supplemental Fig. S4). The above-mentioned peaks were not present in control reactions without LPMO tested for every condition (data not shown). No peaks compatible with C4-oxidation were observed. These results confirmed that recombinant *Ps*AA9A was purified in an active form and that it is a cellulose C1-oxidative enzyme (EC 1.14.99.54).

Electron donors and substrate specificity for *Ps*AA9A

In nature, LPMOs require molecular oxygen and an extracellular electron source, which could be supplied enzymatically, i.e. by cellobiose dehydrogenase (CDH), or by small molecule reductants present in the lignocellulosic biomass. A set of compounds that could act as electron donors was assayed using PASC as substrate and soluble reaction products were analyzed by MALDI-TOF. Control reactions were performed without electron donor and without LPMO, separately. C1-oxidized oligosaccharides were detected when using ascorbic acid and the phenolic compounds gallic acid, pyrogallol, caffeic acid, and ferulic acid but not with *p*-coumaric acid (Supplemental Fig. S5), proving that a wide range of small phenolic compounds could act as electron donors.

For substrate specificity assays, gallic acid was selected as electron donor, as it was previously described to be more stable than ascorbic acid in oxygenated buffers at pH 6 (Kracher et al. 2016). As expected, *Ps*AA9A was active on the cellulosic substrates Avicel (crystalline cellulose) and PASC. However, we also observed activity on squid β-chitin, which

had not been previously reported for AA9 LPMOs (Fig. 3). This activity was also detected when using ascorbic acid as electron donor. Control reactions for β-chitin alone and with electron donor were performed (Supplemental Fig. S6). Other polysaccharide substrates with varying glycosidic linkages were tested including pachyman, glucomannan, galactomannan, lichenan, xyloglucan, xylan from beechwood, and α-chitin, but the release of native and oxidized oligosaccharides was not detected in these cases (Table 1).

*Ps*AA9A boosts the activity of commercial cellulases

In order to test the synergic potential of *Ps*AA9A with cellulases for the deconstruction of cellulose, it was assayed on PASC, in co-incubation experiments with individual commercial cellulases (GH6 cellobiohydrolase II, GH7 cellobiohydrolase I, GH5 endoglucanase, or GH1 β-glucosidase) and the released products were quantified by HPAEC-PAD. The concentration of commercial enzymes was selected to release quantifiable products by themselves, without saturating the reaction, to be able to monitor a potential increase (see materials and methods). Experiments were carried out for 3 h, as COS release was not detected by *Ps*AA9A alone at this time point in a time-course assay (Supplemental Fig. S7). Synergism indexes (SI) were calculated comparing glucose (in the case of GH1) or cellobiose concentration (μM) in the soluble products of the individual and combined reactions. High SI were detected when *Ps*AA9A was co-incubated with GH1, GH5, and GH6, demonstrating a boosting effect in the activity of the individual glycoside hydrolases (Fig. 4a-c). Noteworthy, although there was a boosting effect in cellobiose release when GH7 cellobiohydrolase I was supplemented with *Ps*AA9A, an inhibition was observed in the presence of 1 mM gallic acid (Fig.4d) which can be explained by gallic acid partial inhibition of GH7 activity under the assay conditions (Supplemental Fig. S8).

DISCUSSION

Although an outstanding number of in silico data on fungal genomes, transcriptomes and secretomes have been published in the past decade (Aguilar-Pontes et al. 2014; Grigoriev et al. 2014) the processing and biological analysis of this information is lagging far behind.

The strikingly high representation of AA9s in fungal genomes (Bennati-Granier et al. 2015; Berrin et al. 2017; Berlemont, 2017) and the big sequence diversity found within this family (Vaaje-Kolstad et al. 2017; Frommhagen et al. 2018; Hemsworth et al. 2015) suggests a wide versatility of their mechanism of action and substrate specificity which may result in better adaptations to different environments. Among the seven published LPMO families, proteins of family AA9 show the largest variation in substrate specificity (Frommhagen et al. 2018). Moreover, AA9 LPMOs have different regioselectivities that can generate polysaccharide chain breaks resulting from oxidation at C1, C4, or at both carbon atoms of a sugar ring (Vaaje-Kolstad et al. 2010; Quinlan et al. 2011; Hemsworth et al. 2015).

P. sanguineus has 16 putative AA9 family LPMOs encoded in its genome. Among these, *Ps*AA9A was the only upregulated AA9 transcript when the fungus was grown on wheat straw biomass (Miyauchi et al. 2016) and it is the only one appended to a CBM1. CBM1 modules, which are found almost exclusively in fungi, show affinity towards cellulose but binding to chitin has also been described in one case (Rooijakkers et al. 2018). Previous studies have shown that LPMOs linked to a CBM release more cello-oligosaccharides from cellulose compared to LPMOs without a CBM (Bennati-Granier et al*. 2015;* Crouch et al*. 201*6).

When incubated with the cellulosic substrates (PASC and Avicel), *Ps*AA9A generated native and C1-oxidized cello-oligosaccharides, proving its lytic C1-specific oxidative activity on cellulose. Not surprisingly, sequence alignment and phylogenetic analysis of *Ps*AA9A alongside characterized AA9 LPMOs (reported in CAZY database) placed it in the same cluster as C1-oxidizing fungal AA9 LPMOs *Hi*LPMOB from *H. irregulare* and *Mt*PMO3 from *M. thermophila*, further supporting its mechanism of action. Analysis of the 3D structures of *Hi*LPMOB and *Mt*PMO3 (Liu et al. 2018) revealed certain features that differed from other C1-specific AA9 LPMOs, including an extended L2 loop with two aromatic residues, which are also found in *Ps*AA9A. However, the biological implication of this is still unclear. Further activity analysis and structural studies of a higher number of C1-specific enzymes may clarify whether these features could represent an evolutionary adaptation of a subgroup of C1-specific LPMO to substrate binding, as suggested for *Hi*LPMOB and *Mt*PMO3 (Liu et al. 2018).

To date, activity on cellulose was reported for C1, C4 and C1-C4 oxidizing LPMOs, but activity against other polysaccharides such as xylan and mixed-linkage glucans was only reported for C1-C4 and C4 LPMOs (Liu et al. 2018; Frommhagen et al. 2018;). Enzymes that

oxidize exclusively at C1 have only shown activity on cellulose (Frommhagen et al. 2016; Bennati-Granier et al. 2015; Liu et al. 2017). In this regard, *Ps*AA9A was not active on several non-cellulosic substrates (such as xylan, glucomannan and α-chitin) but we observed peaks compatible with oxidized chito-oligosaccharides (CHOS) with DP 5 to 10 released from squid β-chitin, an activity only reported so far for LPMOs of families AA10, AA11 and AA15, being fungal enzymes exclusively from family AA11 (Vaaje-Kolstad et al. 2019). Nevertheless, further studies will be necessary to confirm and characterize the activity on chitin.

The discovery of LPMOs has had a major impact in the way we understand enzymatic conversion of polysaccharides, mainly due to their ability to boost the activity of classical hydrolytic enzymes by enhancing substrate accessibility (Vaaje-Kolstad et al. 2010; Harris et al. 2010). *Ps*AA9A showed synergistic activity with a commercial GH1 β-glucosidase, a GH5 endoglucanase, and a GH6 cellobiohydrolase II, a result in accordance with previous transcriptomic and secretomic data from biomass-grown fungus (Miyauchi et al. 2016), where *Ps*AA9A was co-expressed with several GHs, including a GH5 and a GH6. We did not observe an increase of GH7 cellobiohydrolase I activity on PASC by addition of *Ps*AA9A when small phenolic electron donor, such as gallic acid, was present. Moreover, GH7 activity was lower in the presence of gallic acid (without *Ps*AA9A). These results were in accordance to previous reports that described the inhibition of GH activity by phenolic compounds (Berlin et al. 2006), which was higher for CBH I than for endoglucanases or β-glucosidases (Guo et al. 2014; Mhlongo et al. 2015). Therefore, boosting with exo-glucanases was higher in the case of non-reducing acting enzymes (such as GH6) than with reducing-end acting enzymes such as GH7, which could have further implications when supplementing fungal enzymatic cocktails that have a high abundance of GH7.

The findings presented in this work are relevant to the better understanding of the complex machinery that *P. sanguineus* utilizes for biomass decomposition, which includes this AA9 LPMO.

DECLARATIONS

Funding

This work was supported by Grants PICT2016-4695 (from the National Agency for Science and Technology Promotion from Argentina, ANPCyT) and Grant 20020130100476BA (from the University of Buenos Aires). The Ultraflex II (Bruker, Billerica, USA) TOF/TOF mass spectrometer was supported by ANPCyT Grant PME 125 (CEQUIBIEM). ML, AC, MPV, SAW and EC are Research Career Scientists of the National Research Council of Argentina (CONICET). NCB and EC acknowledge funding from the N8 AgriFood catalyst programme.

Conflict of interests

The authors declare no financial or commercial conflict of interest.

Availability of data and material

Data of *P. sanguineus* *Ps*AA9A synthetic coding sequence was deposited at DDBJ/EMBL/GenBank under the accession number MT076044.

Code availability

Not applicable.

Authors' contributions

EC, NCB and SW conceived and designed research. MG, ML and FS conducted experiments. PV and AC contributed analytical tools and analyzed data. MG wrote the manuscript. All authors read and approved the manuscript.

AKNOWLEDGEMENTS

Authors thank Dr. Leonardo Gomez and Rachel Hallam for invaluable technical assistance.

REFERENCES

Aachmann FL, Sørlie M, Skjåk-Bræk G, Eijsink VGH, and Vaaje-Kolstad G (2012) NMR structure of a lytic polysaccharide monooxygenase provides insight into copper binding, protein dynamics, and substrate interactions. Proc Natl Acad Sci USA 109(46):18779–18784. http://doi.org/10.1073/pnas.1208822109

Abdul Rahman S, Bergström E, Watson CJ, Wilson KM, Ashford DA, Thomas JR, Ungar D, Thomas-Oates JE (2014) Filter-aided *N*-glycan separation (FANGS): a convenient sample preparation method for mass spectrometric *N*-glycan profiling. J proteome res 13(3):1167–1176. http://doi.org/10.1021/pr401043r

Abuja PM, Schmuck M, Pilz I, Tomme P, Claeyssens M, Esterbauer H (1988) Structural and functional domains of cellobiohydrolase I from *Trichoderma reesei*. Eur Biophys J 15:339-342. http://doi.org/10.1007/BF00254721

Aguilar-Pontes MV, de Vries RP, Zhou M (2014) (Post-)genomics approaches in fungal research. Brief Funct Genomics 13(6):424-439. http://doi.org/10.1093/bfgp/elu028

Alvarado I, Navarro D, Record E, Asther M, Asther M, Lesage-Meessen L (2003) Fungal biotransformation of *p*-coumaric acid into caffeic acid by *Pycnoporus cinnabarinus*: an alternative for producing a strong natural antioxidant. World J Microb Biot 19:157-160. http://doi.org/10.1023/A:1023264200256

Asther M, Lomasco A, Asther S, Moukha S, Lesage-meessen L (1998) Metabolic pathways of biotransformation and biosynthesis of aromatic compounds for flavour industry by the basidiomycete *Pycnoporus cinnabarinus*. Micol Neotrop Apl 11:69-76.

Bennati-Granier C, Garajova S, Champion C, Grisel S, Haon M, Zhou S, Fanuel M, Ropartz D, Rogniaux H, Gimbert I, Record E, Berrin JG (2015) Substrate specificity and regioselectivity of fungal AA9 lytic polysaccharide monooxygenases secreted by *Podospora anserina*. Biotechnol Biofuels 8:90. https://doi.org/10.1186/s13068-015-0274-3

Berlemont R (2017) Distribution and diversity of enzymes for polysaccharide degradation in fungi. Sci Rep 7:222. https://doi.org/10.1038/s41598-017-00258-w

Berlin A, Balakshin M, Gilkes N, Kadla J, Maximenko V, Kubo S, Saddler J (2006) Inhibition of cellulase, xylanase and β-glucosidase activities by softwood lignin preparations. J Biotech 125:198–209. http://doi.org/10.1016/j.jbiotec.2006.02.021

Berrin JG, Rosso MN, Hachem MA (2017) Fungal secretomics to probe the biological functions of lytic polysaccharide monooxygenases. Carbohydr Res 448:155-160. http://doi.org/10.1016/j.carres.2017.05.010

Campos P, Levin L, Wirth S (2016) Heterologous production, characterization and dye decolorization ability of a novel thermostable laccase isoenzyme from *Trametes trogii* BAFC 463. Process Biochem 51: 895–903. http://dx.doi.org/10.1016/j.procbio.2016.03.015

Couturier M, Navarro D, Chevret D, Henrissat B, Piumi F, Ruiz-Dueñas F, Martinez AT, Grigoriev I, Riley R, Lipzen A, Berrin JG, Master E, Rosso MN (2015) Enhanced degradation of softwood versus hardwood by the white-rot fungus *Pycnoporus coccineus*. Biotechnol Biofuels 8:216. http://doi.org/10.1186/s13068-015-0407-8

Crouch LI, Labourel A, Walton PH, Davies GJ, Gilbert HJ (2016) The contribution of non-catalytic carbohydrate binding modules to the activity of lytic polysaccharide monooxygenases. J Biol Chem 291(14):7439–7449. http://doi.org/10.1074/jbc.M115.702365

Eijsink VGH, Petrovic D, Forsberg Z, Mekasha S, Røhr AK, Várnai A, Bissaro B, Vaaje-Kolstad G (2019) On the functional characterization of lytic polysaccharide monooxygenases (LPMOs). Biotechnol Biofuels 12:58. https://doi.org/10.1186/s13068-019-1392-0

Falconnier B, Lapierre C, Lesage-Meessen L, Yonnet G, Brunerie P, Colonna-Ceccaldi B, Corrieu G, Asther M (1994) Vanillin as a product of ferulic acid biotransformation by the white-rot fungus *Pycnoporus cinnabarinus* 1-937: identification of metabolic pathways. J Biotech 37:123-132. http://doi.org/10.1016/0168-1656(94)90003-5

Falkoski DL, Guimarães VM, de Almeida MN, Alfenas AC, Colodette JL, de Rezende ST (2012) Characterization of cellulolytic extract from *Pycnoporus sanguineus* PF-2 and its application in biomass saccharification. Appl Biochem Biotechnol 166:1586–1603. https://doi.org/10.1007/s12010-012-9565-3

Forsberg Z, Vaaje-Kolstad G, Westereng B, Bunæs AC, Stenstrøm Y, MacKenzie A, Sørlie M, Horn SJ, Eijsink VG (2011) Cleavage of cellulose by a CBM33 protein. Protein Sci 20(9):1479-83. http://doi.org/10.1002/pro.689

Frommhagen M, Koetsier MJ, Westphal AH, Visser J, Hinz SW, Vincken JP, van Berkel WJ, Kabel MA, Gruppen H (2016) Lytic polysaccharide monooxygenases from *Myceliophthora thermophila* C1 differ in substrate preference and reducing agent specificity. Biotechnol Biofuels 9(1):186. http://doi.org/10.1186/s13068-016-0594-y

Frommhagen M, Westphal AH, van Berkel WJH, Kabel MA (2018) Distinct substrate specificities and electron‐donating systems of fungal lytic polysaccharide monooxygenases. Front Microbiol 9:1080. http://doi.org/10.3389/fmicb.2018.01080

Gilkes NR, Henrissat B, Kilburn DG, Miller RC Jr, Warren RAJ (1991) Domains in microbial β-1,4-glycanases: sequence conservation, function, and enzyme families. Microbiol Rev 55(2):303-315. PMID: 1886523 PMCID: PMC372816

Grigoriev IV, Nikitin R, Haridas S, Kuo A, Ohm R, Otillar R, Riley R, Salamov A, Zhao X, Korzeniewski F, Smirnova T, Nordberg H, Dubchak I, Shabalov I (2014) MycoCosm portal: gearing up for 1000 fungal genomes. Nucleic Acids Res 42:D699–D704. http://doi.org/10.1093/nar/gkt1183

Guo F, Shi W, Sun W, Li X, Wang F, Zhao J, Qu Y (2014) Differences in the adsorption of enzymes onto lignins from diverse types of lignocellulosic biomass and the underlying mechanism. Biotechnol Biofuels 7(1):38. http://doi.org/doi:10.1186/1754-6834-7-38

Harris PV, Welner D, McFarland KC, Re E, Navarro Poulsen JC, Brown K, Salbo R, Ding H, Vlasenko E, Merino S, Xu F, Cherry J, Larsen S, Lo Leggio L (2010) Stimulation of lignocellulosic biomass hydrolysis by proteins of glycoside hydrolase family 61: structure and function of a large, enigmatic family. Biochemistry 49(15):3305-16. http://doi.org/10.1021/bi100009p

Hemsworth GR, Johnston EM, Davies GJ, Walton PH (2015) Lytic polysaccharide monooxygenases in biomass conversion. Trends Biotechnol 33(12):747-761. http://doi.org/10.1016/j.tibtech.2015.09.006

Jagadeeswaran G, Gainey L,Mort AJ (2018) An AA9-LPMO containing a CBM1 domain in *Aspergillus nidulans* is active on cellulose and cleaves cello-oligosaccharides. AMB Expr 8:171. http://doi.org/10.1186/s13568-018-0701-5

Karkehabadi S, Hansson H, Kim S, Piens K, Mitchinson C and Sandgren M (2008) The first structure of a glycoside hydrolase family 61 member, Cel61B from *Hypocrea jecorina*, at 1.6 Å resolution. J Mol Biol 383:144–154. https://doi.org/10.1016/j.jmb.2008.08.016

Kobayashi K, Sumitomo H, Ina Y (1985) Synthesis and functions of polystyrene derivatives having pendant oligosaccharides. Polym J 17:567–575. https://doi.org/10.1295/polymj.17.567

Kobayashi K, Kamiya S, Enomoto N (1996) Amylose-carrying styrene macromonomer and its homo- and copolymers: synthesis via enzyme-catalyzed polymerization and complex formation with iodine. Macromolecules 29(27):8670-8676. http://doi.org/10.1021/ma9603443

Kracher D, Scheiblbrandner S, Felice AK, Breslmayr E, Preims M, Ludwicka K, Haltrich D, Eijsink VG, Ludwig R (2016) Extracellular electron transfer systems fuel cellulose oxidative degradation. Science 352:1098-1101. http://doi.org/10.1126/science.aaf3165

Langsford ML, Gilkes NR, Singh B, Moser B, Miller RC Jr, Warren RA, Kilburn DG (1987) Glycosylation of bacterial cellulases prevents proteolytic cleavage between functional domains. FEBS Lett 225(1-2):163-7. http://doi.org/10.1016/0014-5793(87)81150-x

Levasseur A, Drula E, Lombard V, Coutinho PM, Henrissat B (2013) Expansion of the enzymatic repertoire of the CAZy database to integrate auxiliary redox enzymes. Biotechnol Biofuels 6:41. https://doi.org/10.1186/1754-6834-6-41

Levasseur A, Lomascolo A, Chabrol O, Ruiz-Dueñas FJ, Boukhris-Uzan E, Piumi F, Kües U, Ram AF, Murat C, Haon M, Benoit I, Arfi Y, Chevret D, Drula E, Kwon MJ, Gouret P, Lesage-Meessen L, Lombard V, Mariette J, Noirot C, Park J, Patyshakuliyeva A, Sigoillot JC, Wiebenga A, Wösten HA, Martin F, Coutinho PM, de Vries RP, Martínez AT, Klopp C, Pontarotti P, Henrissat B, Record E (2014) The genome of the white-rot fungus *Pycnoporus cinnabarinus*: a basidiomycete model with a versatile arsenal for lignocellulosic biomass breakdown. BMC Genomics 15:486. http://doi.org/10.1186/1471-2164-15-486

Levin L, Villalba L, Da Re V, Forchiassin F, Papinutti L (2007) Comparative studies of loblolly pine biodegradation and enzyme production by Argentinean white rot fungi focused on biopulping processes. Process Biochem 42:995–1002. https://doi.org/10.1016/j.procbio.2007.03.008

Li X, Beeson WT, Phillips CM, Marletta MS, Cate JHD (2012) Structural basis for substrate targeting and catalysis by fungal polysaccharide monooxygenases. Structure 20:1051–1061. http://doi.org/10.1016/j.str.2012.04.002

Linder S, Schliwa M, Kube-Granderath E (1996) Direct PCR screening of *Pichia pastoris* clones. Biotechniques 20:980-982. https://doi.org/10.2144/96206bm08

Liu B, Olson Å, Wu M, Broberg A, Sandgren M (2017) Biochemical studies of two lytic polysaccharide monooxygenases from the white-rot fungus *Heterobasidion irregulare* and their roles in lignocellulose degradation. PLoS One 12(12). http://doi.org/10.1371/journal.pone.0189479

Liu B, Kognole AA, Wu M, Westereng B, Crowley MF, Kim S, Dimarogona M, Payne CM, Sandgren M (2018) Structural and molecular dynamics studies of a C1-oxidizing lytic polysaccharide monooxygenase from *Heterobasidion irregulare* reveal amino acids important for substrate recognition. FEBS Journal 285:2225–2242. http://doi.org/10.1111/febs.14472

Lomascolo A, Uzan-Boukhris E, Herpoël-Gimbert I, Sigoillot JC, Lesage-Meessen L (2011) Peculiarities of *Pycnoporus* species for applications in biotechnology. Appl Microbiol Biotechnol 92:1129–1149. https://doi.org/10.1007/s00253-011-3596-5

Lundell TK, Mäkelä MR, Hildén K (2010) Lignin-modifying enzymes in filamentous basidiomycetes - ecological, functional and phylogenetic review. J Basic Microbiol 50(1): 5–20. http://doi.org/10.1002/jobm.200900338

Mhlongo SI, den Haan R, Viljoen-Bloom M, van Zyl WH (2015) Lignocellulosic hydrolysate inhibitors selectively inhibit/deactivate cellulase performance. Enzyme Microb Tech 81:16–22. http://doi.org/10.1016/j.enzmictec.2015.07.005

Miyauchi S, Navarro D, Grigoriev IV, Lipzen A, Riley R, Chevret D,Grisel S, Berrin J-G, Henrissat B, Rosso M-N (2016) Visual comparative omics of fungi for plant biomass deconstruction. Front Microbiol 7:1335. https://doi.org/10.3389/fmicb.2016.01335

Miyauchi S, Navarro D, Grisel S, Chevret D, Berrin J-G, Rosso M-N (2017) The integrative omics of white-rot fungus *Pycnoporus coccineus* reveals co-regulated CAZymes for orchestrated lignocellulose breakdown. PLoS ONE 12(4):e0175528. https://doi.org/10.1371/journal. pone.0175528

Moses V, Hatherley R, Bishop OT (2016) Bioinformatic characterization of type-specifc sequence and structural features in auxiliary activity family 9 proteins. Biotechnol Biofuels 9:239. http://doi.org/10.1186/s13068-016-0655-2

Müller G, Várnai A, Salomon Johansen K, Eijsink VGH and Horn SJ (2015) Harnessing the potential of LPMO-containing cellulase cocktails poses new demands on processing conditions. Biotechnol Biofuels 8:187. http://doi.org/10.1186/s13068-015-0376-y

Niderhaus N, Garrido M, Insani M, Campos E, Wirth SA (2018) Heterologous production and characterization of a thermostable GH10 family endo-xylanase from *Pycnoporus sanguineus* BAFC 2126. Proc Bio 67:92–98. https://doi.org/10.1016/j.procbio.2018.01.017

Quinlan RJ, Sweeney MD, Lo Leggio L, Otten H, Poulsen JC, Johansen KS, Krogh KB, Jørgensen CI, Tovborg M, Anthonsen A, Tryfona T, Walter CP, Dupree P, Xu F, Davies GJ, Walton PH (2011) Insights into the oxidative degradation of cellulose by a copper metalloenzyme that exploits biomass components. Proc Natl Acad Sci USA108(37):15079-84. http://doi.org/10.1073/pnas.1105776108

Robert X, Gouet P (2014) Deciphering key features in protein structures with the new ENDscript server. Nucleic Acids Res 42:W320-W324. http://doi.org/10.1093/nar/gku316

Rohr CO, Levin LN, Mentaberry AN, Wirth SA (2013) A first insight into *Pycnoporus sanguineus* BAFC 2126 transcriptome. PLoS One 8(12):e81033. http://doi.org/10.1371/journal.pone.0081033

Rooijakkers BJM, Ikonen MS, Linder MB (2018) Fungal-type carbohydrate binding modules from the coccolithophore *Emiliania huxleyi* show binding affinity to cellulose and chitin. PLoS One 13(5):e0197875. http://doi.org/10.1371/journal.pone.0197875

Sabbadin F, Hemsworth GR, Ciano L, Henrissat B, Dupree P, Tryfona T, Marques R, Sweeney ST, Besser K, Elias L, Pesante G, Li Y, Dowle AA, Bates R, Gomez LD, Simister R, Davies GJ, Walton PH, Bruce NC, McQueen-Mason SJ (2018) An ancient family of lytic polysaccharide monooxygenases with roles in arthropod development and biomass digestion. Nat Commun 9:756. https://doi.org/10.1038/s41467-018-03142-x

Tamura K, Stecher G, Peterson D, Filipski A, and Kumar S (2013) MEGA6: molecular evolutionary genetics analysis version 6.0. Mol Biol Evol 30:2725-2729. http://doi.org./10.1093/molbev/mst197

Vaaje-Kolstad G, Westereng B, Horn SJ, Liu Z, Zhai H, Sørlie M, Eijsink VG (2010) An oxidative enzyme boosting the enzymatic conversion of recalcitrant polysaccharides. Science 30(6001):219-22. http://doi.org/10.1126/science.1192231

Vaaje-Kolstad G, Forsberg Z, Loose JSM, Bissaro B and Eijsink VGH (2017) Structural diversity of lytic polysaccharide monooxygenases. Curr Opin Struc Biol 44:67–76. http://dx.doi.org/10.1016/j.sbi.2016.12.012

Vaaje-Kolstad G, Tuveng TR, Mekasha S, and Eijsink, VGH (2019) Enzymes for modification of chitin and chitosan. In: L.A. Broek and C.G. Boeriu (eds) Chitin and chitosan: properties and applications, Wiley, New York, pp 189-228. http://doi.org/10.1002/9781119450467.ch8

Várnai A, Mäkelä MR, Djajadi DT, Rahikainen J, Hatakka A, Viikari L (2014) Carbohydrate-binding modules of fungal cellulases: occurrence in nature, function, and relevance in industrial biomass conversion. Adv Appl Microbiol 88:103-165. http://doi.org/10.1016/B978-0-12-800260-5.00004-8

Zhang J, Silverstein KAT, Castaño JD, Figueroa M, Schilling JS (2019) Gene regulation shifts shed light on fungal adaption in plant biomass decomposers. MBio 10:e02176-19. https://doi.org/10.1128/mBio.02176-19

FIGURE LEGENDS

Fig. 1 In silico analysis of *Ps*AA9A. Three-dimensional structure of *Ps*AA9A catalytic module. The catalytic residues His 1, His 80 and Tyr 167 are highlighted in violet and the copper atom is shown as a green sphere. Tyrosine residues 20 and 36, located in the substrate binding surface, are highlighted in orange. This image was made with VMD software support. VMD is developed with NIH support by the Theoretical and Computational Biophysics group at the Beckman Institute, University of Illinois at Urbana-Champaign **(A)**. Phylogenetic tree constructed using Neighbor Joining statistical method. The optimal tree is drawn to scale and the percentage of replicate trees in which the associated sequences clustered together in the boostrap test (1000 replicates) are shown next to the branches. *Ps*AA9A is highlighted in blue.

NCBI GenBank accession numbers for each sequence are indicated between parenthesis **(B)**. Phylogenetic and molecular evolutionary analyses were conducted using MEGA version 6 (Tamura et al. 2013)

Fig. 2 HPAEC-PAD and MALDI-TOF analysis of the glucan products after treating PASC with *Ps*AA9A. HPAEC-PAD overlapped chromatograms of products obtained after incubation of 0.5% PASC with (blue) and without (black) 2 µM *Ps*AA9A and 1 mM ascorbic acid for 24 h **(A)**. MALDI-TOF spectra of products obtained under the same reaction conditions **(B)**. Glc_n stands for native cello-oligosaccharides and Glc_n-GlcA represents C1 oxidized aldonic sugars. The main peaks correspond to mono- or di- sodiated adducts of C1 aldonic acids, imparting +16 and +38 units respectively, relative to the mono-sodiated unoxidized form. DP: degree of polymerization; a.u.: arbitrary unit. HPAEC-PAD standards: Identity of Glc_n was assigned by commercial standards, Gcl-GclA by an in-house standard, and $Glc_{(2-5)}$-GlcA were inferred from retention times of previous references

Fig. 3 MALDI-TOF analysis of the glucan products after treating Avicel and β-chitin with *Ps*AA9A. MALDI-TOF spectra in positive ion mode showing native and oxidized oligosaccharides obtained after incubation of 0.4% avicel **(A)** and β-chitin **(B)** with 2 µM *Ps*AA9A and 4 mM ascorbic acid for 24 h. Incubation of 0.4% avicel and β-chitin with 2 µM *Ps*AA9A in the absence of the electron donor are shown in **(C)** and **(D)**, respectively. For both substrates, the main signals correspond to native oligosaccharides and mono- or di- sodiated adducts of C1 aldonic acids, imparting +16 and +38 units respectively, relative to the mono-sodiated unoxidized form. Smaller signals for the mono-sodiated lactone (-2 units from the unoxidized form) were also identified. DP: degree of polymerization; a.u.: arbitrary unit

Fig. 4 Combined activity of *Ps*AA9A with commercial GHs. Quantification by HPAEC-PAD analysis, showing the release of glucose by a commercial GH1 **(A)** and cellobiose by commercial GH5 **(B),** GH6 **(C)**, and GH7 **(D)** from 0.4% PASC over 3h at 30°C, in presence (+) or absence (-) of *Ps*AA9A and/or gallic acid. SI stands for Synergism Index, calculated as the glucan release by GH + *Ps*AA9A + gallic acid (black bar)/ glucan release by GH + gallic acid (white bar). Bars indicate means (error bars: standard deviations of three replicates). The identity and quantity of each species was determined by analysis of commercial standards. Tukey test was performed to determine significant differences between means (asterisks)

TABLES

Table 1 *Ps*AA9A substrate specificity analysis. *Ps*AA9A (2 µM) was incubated with different substrates in the presence of 4 mM ascorbic acid at 30°C, pH 6 for 24 h. Soluble products were analyzed by MS MALDI-TOF and the presence (+) or absence (-) of peaks corresponding to native and oxidized COS is reported under "Oligosaccharide detection"

Substrate	Main chain glycosidic linkages	Ramification glycosidic linkages	Oligosaccharide detection
Avicel	$[-Glc\beta\text{-}1,4-]_n$	-	+
PASC	$[-Glc\beta\text{-}1,4-]_n$	-	+
Glucomannan	$[-Man\beta\text{-}1,4Man\beta\text{-}1,4Glc\beta\text{-}1,4-]_n$	-	-
Pachyman	$[-Glc\beta\text{-}1,3-]_n$	-	-
Lichenan	$[Glc\beta\text{-}1,4\text{-}Glc\beta\text{-}1,3\text{-}Glc\beta\text{-}1,4]_n$	-	-
Galactomannan	$[-Man\beta\text{-}1,4-]_n$	Galα-1,6-Man	-
Xyloglucan	$[-Glc\beta\text{-}1,4-]_n$	Galβ-1,2-Xylα-1,6-Glc; Xylα-1,6-Glc	-
Xylan from beechwood	$[-Xyl\beta\text{-}1,4-]_n$	OMe-4-GlcAα-1,2-Xyl	-
α-Chitin (shrimp)	$[GlcNAc\alpha\text{-}1,4]_n$	-	-
β-Chitin (squid)	$[GlcNAc\beta\text{-}1,4]_n$	-	+

Figure 1

Fig.1

A

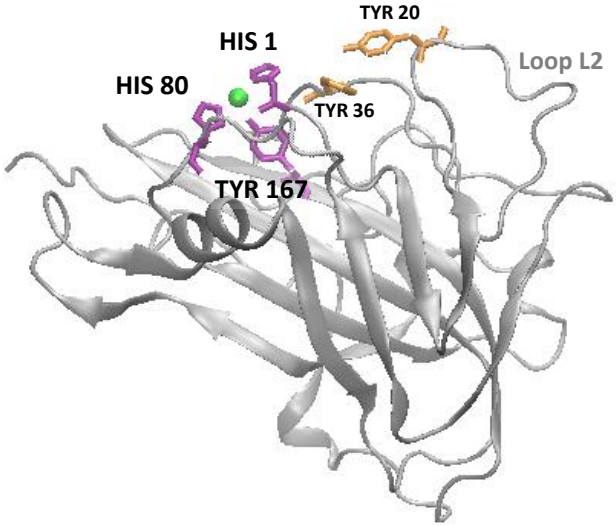

B

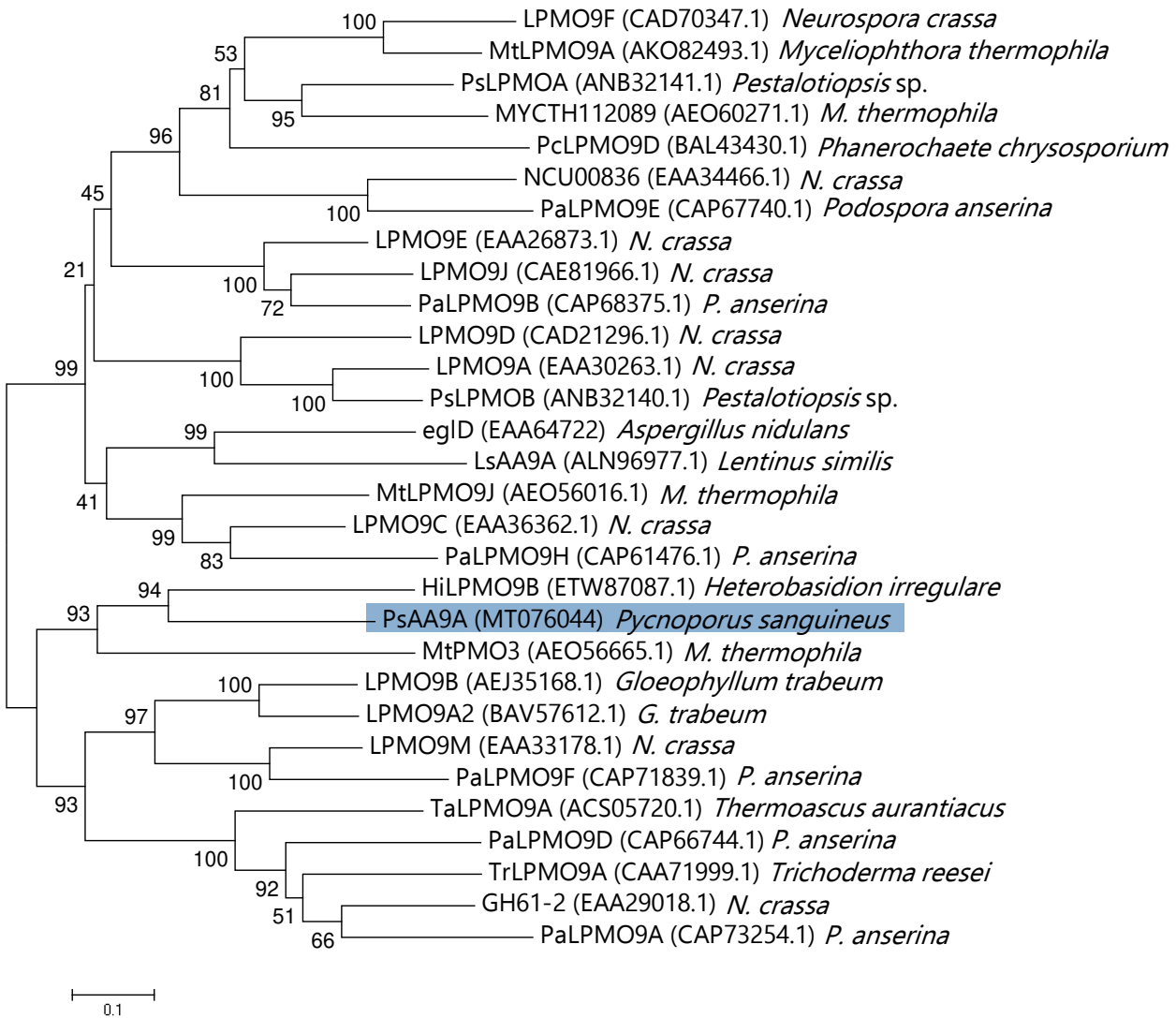

Figure 2

Fig. 2

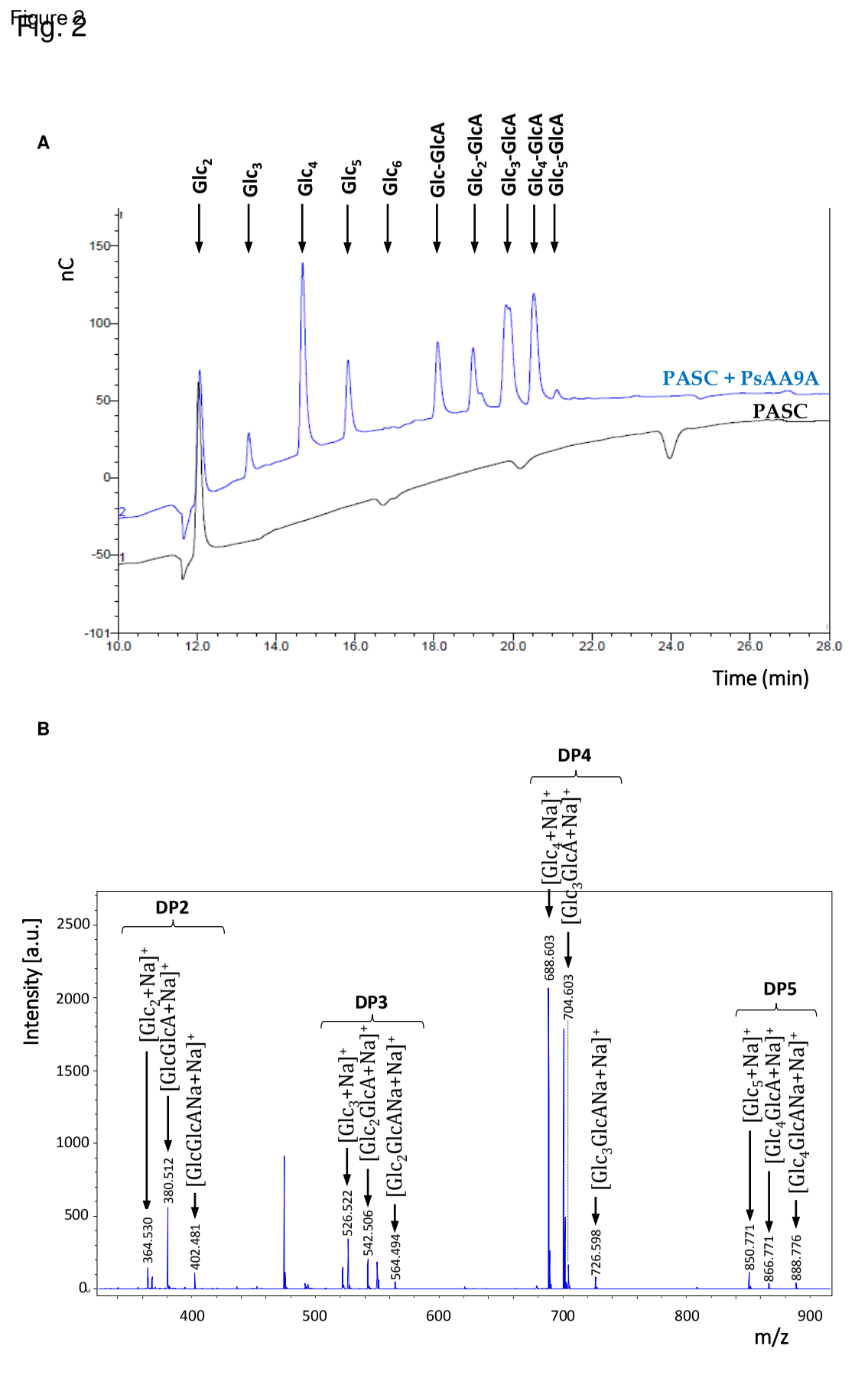

Figure 3

Fig. 3

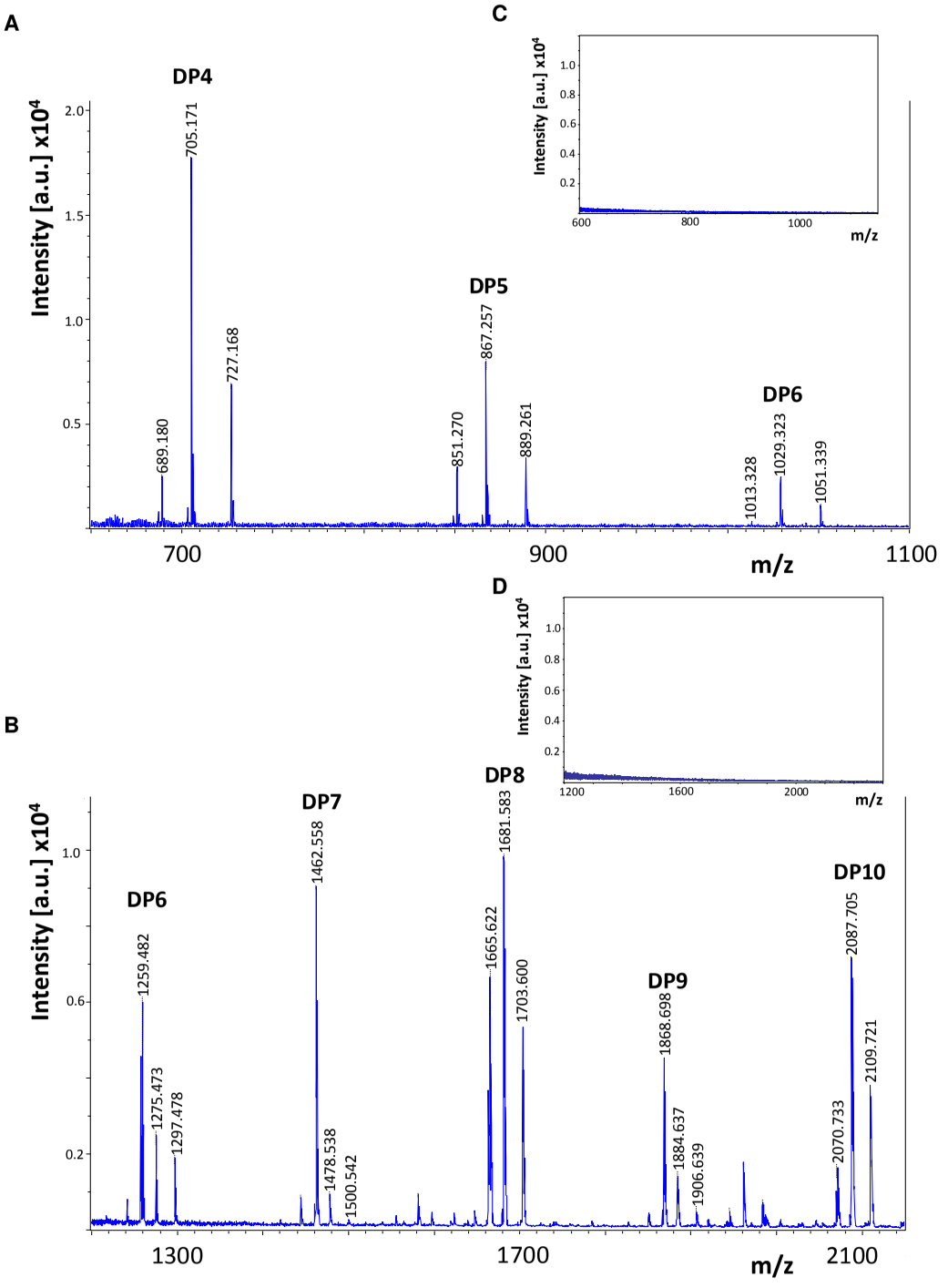

Figure 4
Fig. 4